

Pseudospectra of holographic diffusion: gauge fields breaking free from the master scalar

David Garcia-Fariña,^{1,2} **Karl Landsteiner**,¹ **Pau G. Romeu**,^{1,2} **Pablo Saura-Bastida**^{1,3}

¹*Instituto de Física Teórica UAM/CSIC, Calle Nicolás Cabrera 13-15, 28049 Madrid, Spain*

²*Departamento de Física Teórica, Universidad Autónoma de Madrid, Campus de Cantoblanco, 28049 Madrid, Spain*

³*Departamento de Automática, Ingeniería Eléctrica y Tecnología Electrónica, Universidad Politécnica de Cartagena, Calle Dr. Fleming, S/N, 30202 Cartagena, Murcia*

E-mail: david.garciafarinna@estudiante.uam.es,
karl.landsteiner@csic.es, pau.garcia@uam.es, pablo.saura@upct.es

ABSTRACT: We study pseudospectra of quasinormal frequencies and complex linear momenta of a U(1) gauge field in a Schwarzschild black branes in Anti-de Sitter. We present a novel approach for computing the pseudospectra which uses directly the gauge field variables and contrast it to a conventional master scalar field approach. Upon clarifying a subtlety in the energy norm of the master scalar we show that the pseudospectra of both approaches coincide. In the hydrodynamic regime we find that the hydrodynamic quasinormal frequency, the diffusive mode, is spectrally stable to a very good approximation. On the other hand hydrodynamic complex linear momenta show enhanced spectral instability as a consequence of a pole-collision at zero frequency.

Contents

1	Introduction	1
2	Pseudospectra and stability	5
2.1	Pseudospectra of rectangular matrices	7
2.1.1	An example	9
3	Longitudinal gauge field	11
3.1	Modifications for CLMs	15
4	Master scalar	17
4.1	Boundary Conditions	18
4.2	Energy Norm	18
5	Hodge duality	19
5.1	CLMs from Hodge duality	21
6	Holographic setup	22
6.1	CLMs of $SAdS_{5+1}$ black brane	22
6.1.1	Boundary conditions in the GF framework	22
6.1.2	Setup in the MS framework	23
6.1.3	Numerical results	24
6.2	QNFs of $SAdS_{5+1}$ black brane	27
6.2.1	Boundary conditions in the GF framework	28
6.2.2	Boundary conditions in the MS framework	28
6.2.3	Numerical results	29
6.3	CLMs of $SAdS_{4+1}$ black brane	32
6.3.1	Boundary conditions in the GF framework	32
6.3.2	Setup in the MS framework	33
6.3.3	Numerical results	33
6.4	QNFs of $SAdS_{4+1}$ black brane	35
6.4.1	Boundary conditions in the GF framework	35
6.4.2	Boundary conditions in the MS framework	37
6.4.3	Numerical results	37
6.5	QNFs of $SAdS_{4+1}$ black hole	38
6.5.1	Boundary conditions in the GF framework	40
6.5.2	Boundary conditions in the MS framework	41
6.5.3	Numerical results	41
7	Conclusions and outlook	42

A Stability of general eigenvalue problems	43
B Numerical methods	46
C Convergence of the relative difference between MS and GF approaches for AdS₄₊₁	47
D Convergence tests for QNFs and CLMs	47

1 Introduction

Eigenvalue problems for linear operators are ubiquitous in all of physics, playing a fundamental role in our understanding of both classical and quantum systems. For conservative systems, the corresponding linear operators are self-adjoint. This ensures that eigenvalue analysis is sufficient to understand the dynamics associated with these linear operators. Moreover, under small perturbations of the operators the effect on the eigenvalues will also be small. This allows us to disregard small contributions and use simplified models while keeping control of the effect of the discarded terms. On the other hand, non-conservative systems are characterized by non-self-adjoint and potentially non-normal operators. The existence of non-normality drastically changes the above picture as eigenvalues are no longer stable and very small perturbations to the operators can change them dramatically. Modeling non-conservative systems is therefore much more difficult since approximations might have large effects. Moreover, eigenvalues do not completely characterize a non-normal operator. It is necessary to also address their stability properties.

The standard way to quantify spectral stability is by studying pseudospectra [1–3], which give bounds on the maximal displacement eigenvalues can suffer under arbitrary perturbations of a given size. Unlike eigenvalues, pseudospectra crucially depend on a norm. This is quite natural as in order to assess stability it is necessary to be able to measure sizes. It is crucial to choose a norm that captures the correct physical notion of size for the system. It has been argued, that from a physical standpoint the norm should be a functional reproducing the energy of the eigenfunctions [1].

In the context of gravitational physics, non-self-adjoint operators naturally appear in the study of quasinormal modes (QNMs) of black holes [4–6]. In these geometries the presence of an event horizon acting as a perfectly absorbing membrane renders the time evolution of fluctuations non-conservative. The generator of time-translations, whose eigenvalues are the quasinormal frequencies (QNFs), is a non-self-adjoint differential operator. In asymptotically flat spacetimes, fluctuations

are also outgoing at null infinity, further contributing to the non-self-adjointness. Guided by the above reasoning, in [7] the study of pseudospectra of black holes QNMs was pioneered, finding that the QNFs of a Schwarzschild black hole are unstable. Since then, this same type of instability has also been observed in other asymptotically flat black holes in [8–16] (see [17, 18] also for horizonless compact objects and [19–21] for black holes beyond General Relativity), as well as in de Sitter (dS) [22–24] and anti-de Sitter (AdS) [25–29] geometries. Further studies have also covered the implications of this spectral instability on the strong cosmic censorship [30] and on the gravitational waves emitted in black hole mergers [31, 32]. The stability of full transmission modes was also recently discussed in [33]. Alternatively to QNFs one can also study complex momentum modes in which the frequency is kept real and one solves for complex (angular) momentum. In asymptotically flat spacetimes these are Regge poles [34] and in asymptotically AdS they describe absorption lengths [35]. Spectral stability of such modes has been discussed in [36–42].

Gauge/gravity duality [43–47] postulates that black hole geometries in asymptotically AdS spacetimes are dual to thermal states in a strongly coupled quantum field theory. In this context, black hole quasinormal frequencies are interpreted as poles of retarded propagators of the thermal field theory at real momentum k [48–50]. Consequently, the study of quasinormal frequencies in AdS black holes has led to important insights into hydrodynamics and transport theory in the relativistic regime [51–53], with some remarkable results being the extremely low specific shear viscosity of holographic models of the quark-gluon plasma [54], phase transitions towards superconducting states [55–58] and strongly coupled quantum critical phases [59–61]. Quasinormal modes also play an important role in quantum chaos [62, 63] via the pole skipping phenomenon [64]. Understanding the stability of QNFs in AdS is therefore crucial for its potential implications for strongly coupled plasmas.

Characterizing the stability of those QNFs that vanish as the momentum goes to zero (hydrodynamic QNFs) is of central importance. From the dual QFT perspective, these QNFs are related to conserved charges associated with global symmetries. They dominate the dynamics at large scales in the hydrodynamic regime and are believed to be universal features of the theory. The presence of spectral instability would then challenge this view and thus should be studied carefully.

In this paper we consider the simplest setup containing hydrodynamic modes, the longitudinal sector of a $U(1)$ gauge field with standard Maxwell action

$$S = -\frac{1}{4} \int d^{d+1}x \sqrt{-g} F_{MN} F^{MN}, \quad (1.1)$$

in a Schwarzschild AdS _{$d+1$} black brane described by the following metric in regular

coordinates

$$ds^2 = \frac{l^2}{(1-\rho)^2} \left[-f dt^2 + 2(1-f) dt d\rho + (2-f) d\rho^2 + dy_1^2 + d\mathbf{y}_\perp^2 \right], \quad (1.2)$$

$$f = 1 - (1-\rho)^d,$$

where l is the AdS length scale, which we set to unity without loss of generality, and y_1 and y_\perp are coordinates parallel and perpendicular to the momentum, respectively. In these coordinates, the event horizon lies at $\rho = 0$ and the AdS boundary at $\rho = 1$. We have used the conformal symmetry of the dual QFT to set the temperature $T = d/(4\pi)$. The longitudinal gauge field sector contains a hydrodynamic QNF associated with diffusion of the U(1) charge in the dual QFT. The standard way to treat this sector is to introduce an effective scalar field in two dimensions, called master scalar, which on-shell is equivalent to the above gauge field. Pseudospectra for the master scalar are constructed by writing the scalar equations of motion as an eigenvalue problem and by introducing a norm given by the energy of the two-dimensional master scalar on a constant time slice. This is the approach followed in [26], where the authors studied the gravitoelectric sector of a Reissner-Nordström black brane. It is however not immediately clear if the energy norm of the master scalar and the associated field space captures all the relevant off-shell field configurations of the gauge field. For this reason we introduce a novel approach in which we work directly in terms of the gauge field. This allows us to employ as our energy norm the energy of the Maxwell field on a constant time slice, thus avoiding potential pitfalls. We claim that this approach is more fundamental as it does not require the use of the master scalar. Moreover, this ensures that our approach can be extended to more complicated setups where a master scalar is not easily available. This is indeed the case when we study the pseudospectra of complex momentum modes.

We find that both frameworks, the one based on the master scalar (MS) and the one where we work directly with the gauge field (GF) can be related using Hodge duality and are thus equivalent as long as one is careful with boundary terms in the energy norm for the MS. For any number of dimensions, the original problem of the longitudinal gauge field can be consistently reduced to an equivalent problem of a longitudinal gauge field in an effective 3-dimensional spacetime. Hodge duality in this 3-dimensional spacetime implies that the dynamics of the gauge field should be equivalent to those of a massless scalar living in the same 3-dimensional spacetime. The problem of studying the stability of the Hodge dual scalar field can be seen to be equivalent to the problem formulated in the MS framework, up a boundary term living in the AdS boundary that appears in the energy norm. Whenever this boundary term does not vanish on the space of functions, the MS energy norm fails to be positive definite and thus we claim that in those cases one should instead take the energy norm defined via the Hodge dual field as it is more fundamental.

We observe that although the non-hydrodynamic QNFs are generically unstable, the hydrodynamic one is increasingly stable at low momenta. This indicates that the hydrodynamic description of the system is robust under perturbations, in agreement with the physical expectation that the hydrodynamic description should be universal and thus not excessively sensitive to small perturbations.

A main point of this paper is the stability of complex linear momenta (CLMs) for the longitudinal $U(1)$ gauge field. While QNFs are eigenvalues of the generator of time translations, CLMs correspond to eigenvalues of the generator of spatial translations along some direction parallel to the brane. QNFs and CLMs are dual to poles of the retarded Green's function at fixed momentum (relaxation times) and fixed frequency (absorption lengths), respectively. CLMs also play an essential role in studying causality of the boundary field theory [65, 66]. At zero frequency, the non-hydrodynamic CLMs are dual to the glueball masses of a dimensionally compactified toy model for QCD [67–71]. CLMs have also appeared in the holographic context in [72–75].

The study of the pseudospectra of CLMs of a scalar field in an AdS_{4+1} black brane was carried out in [39]. There, it was found that CLMs are generically more stable than QNFs. Moreover CLM pseudospectra avoid the non-convergence problem present for QNF pseudospectra¹. We find CLM pseudospectra to be convergent. However, we find that while non-hydro CLMs are more stable than non-hydro QNFs, the hydrodynamic CLMs are increasingly unstable as we approach the hydrodynamic regime. This suggests that the hydrodynamic description in the CLM picture is unstable while in the QNF picture it is stable. Although this seems puzzling at first we argue that it is what one should expect. In the CLM picture the two hydrodynamic CLMs behave at small frequency as $k_{\pm} \propto \pm\sqrt{i\omega}$ indicating that collide at zero frequency forming an exceptional point. Exceptional points are characterized by their increased spectral instability [77] and thus we find that the hydro CLMs are unstable as we approach the hydrodynamic regime. Hence the instability of the hydro CLMs is signaling that in the vicinity of pole collisions there is an enhancement in spectral instability. On the other hand, for the hydro QNF there is no pole collision in the hydrodynamic regime and thus no enhancement in instability. Then, both pictures are consistent with the hydrodynamic description. Hydrodynamics predicts a pole collision for the CLMs which in turn results in them being unstable, while in the QNF picture as there is no pole collision the hydro QNF is stable. The different stability properties found for the hydrodynamic mode depending on whether we describe it via QNFs or CLMs agree with the observation of [39] that stability properties of QNFs and CLMs are fundamentally different. From a physical standpoint perturbing while keeping the frequency fixed (CLM picture) is fundamentally different from

¹Pseudospectra for QNFs do not converge in the energy norm for points sufficiently deep in the lower complex half plane in the limit $N \rightarrow \infty$ where N is the gridsize of a given discretization via pseudospectral methods. For details on this see [17, 76].

perturbing with fixed momentum (QNF picture) and thus one generically expects to find nonequivalent stability properties as we do. This behavior is not specific to the black hole realization but an expected generic feature of the diffusion mode.

The paper is organized as follows. We begin in section 2 with a brief review of pseudospectrum drawing heavily from [1]. We pay special attention to the pseudospectra of rectangular matrices which plays a central role in our novel formulation of pseudospectra based on gauge field components, which we discuss in section 3. In section 4 we review the master scalar approach to pseudospectra of QNFs and discuss the associated energy norm.

In section 5 we comment on how 3-dimensional Hodge duality offers a natural way to introduce the master scalar and its positive definite energy norm. We also show how to compute CLMs pseudospectra in the master scalar framework.

We present our results and give details on the boundary conditions in section 6. We discuss pseudospectra of CLMs and QNFs for the black branes of equation (1.2) in 6 and 5 dimensions. We also showcase the validity of our formulation for spherical black holes by computing pseudospectra of QNFs of an AdS_{4+1} black hole in subsection 6.5. In section 7 we summarize our findings, present our conclusions and give an outlook on further studies.

Some remarks on the subtleties arising when dealing with pseudospectra of generalized eigenvalue problems are given in appendix A. Further details on the numerical methods are provided in appendix B. Lastly, in appendices C-D we present some relevant convergence tests.

2 Pseudospectra and stability

In this section we summarize some important definitions and results concerning pseudospectra and condition numbers, and their relevance for the study of the spectral stability of matrices such as the ones arising from the discretization of differential operators. We refer the reader to [1] for further details and for the generalization to operators on infinite-dimensional Hilbert spaces.

Given a square matrix $M \in \mathbb{C}^{N \times N}$, its spectrum $\sigma(M)$ is given by the set of eigenvalues $\{\lambda_i\}$ solutions to the equation

$$(M - \lambda_i \mathbb{I})u_i = 0, \quad (2.1)$$

with u_i the corresponding eigenvector. Alternatively, the spectrum of a generic operator can be defined as the set of points $z \in \mathbb{C}$ where the the resolvent $\mathcal{R}(M; z) = (M - z\mathbb{I})^{-1}$ is not defined. For matrices both definitions are equivalent, although this is not generally the case for arbitrary operators.

An important property of eigenvalues is that for self-adjoint matrices (or, in more physical terms, conservative systems), the spectral theorem ensures that if we

perturb the system with a perturbation of size ε the eigenvalues of the perturbed operator cannot suffer a displacement greater than ε [78, 79]. This property holds in general for any normal matrix M satisfying $[M, M^\dagger] = 0$. Let us briefly explain our notation: we denote the complex conjugate with a bar, complex conjugate transpose with an asterisk and adjoint, defined as $\langle M^\dagger u, v \rangle = \langle u, Mv \rangle$, with a dagger.

However, in non-conservative systems normality is not guaranteed and small perturbations could potentially alter the spectrum in a significant manner. For that reason, one concludes [1] that in non-conservative systems eigenvalue analysis alone is insufficient as the spectrum might be unstable.

To probe the stability of eigenvalues one introduces the notion of ε -pseudospectrum, which can be defined in three mathematically equivalent ways [1]:

Def. 2.1 (Resolvent norm approach) *Given a square matrix $M \in \mathbb{C}^{N \times N}$, and $\varepsilon > 0$, the ε -pseudospectrum $\sigma_\varepsilon(M)$ is*

$$\sigma_\varepsilon(M) = \{z \in \mathbb{C} : \|\mathcal{R}(z; M)\| > 1/\varepsilon\}, \quad (2.2)$$

with the convention $\|\mathcal{R}(z; M)\| = \infty$ for $z \in \sigma(M)$.

Def. 2.2 (Perturbative approach) *Given a square matrix $M \in \mathbb{C}^{N \times N}$, and $\varepsilon > 0$, the ε -pseudospectrum $\sigma_\varepsilon(M)$ is*

$$\sigma_\varepsilon(M) = \{z \in \mathbb{C}, \exists V, \|V\| < \varepsilon : z \in \sigma(M + V)\}. \quad (2.3)$$

Def. 2.3 (Pseudoeigenvalue approach) *Given square matrix $M \in \mathbb{C}^{N \times N}$, and $\varepsilon > 0$, the ε -pseudospectrum $\sigma_\varepsilon(M)$ is*

$$\sigma_\varepsilon(M) = \{z \in \mathbb{C}, \exists u^\varepsilon \in \mathbb{C}^N : \|(M - z\mathbb{I})u^\varepsilon\| < \varepsilon\|u^\varepsilon\|\}, \quad (2.4)$$

where u^ε is a ε -pseudoeigenvector with ε -pseudoeigenvalue z .

Note that, contrary to the spectrum, the pseudospectrum depends on the operator norm

$$\|V\| = \max_{u \in \mathbb{C}^N} \frac{\|Vu\|}{\|u\|}, \quad (2.5)$$

as, in order to quantify stability, it needs a notion of what constitutes a small perturbation.

Remarkably, definition 2.2 corresponds to the physical intuition we were seeking: the ε -pseudospectrum constitutes the maximal region containing all possible displacements of the eigenvalues under perturbations of size ε . It is then quite natural to represent the pseudospectrum as a contour map indicating the boundaries of these regions for multiple values of ε . However, computationally definition 2.2 is very inefficient as one should compute the spectra for all possible bounded perturbations.

For that reason, when studying general instability properties one instead uses definition 2.1 which, despite lacking such a clear physical interpretation, is much more manageable to compute in a finite-dimensional setting such as the ones arising when employing numerical approximations to the operators.

Another useful tool for studying the stability of eigenvalues is the set of condition numbers $\{\kappa_i\}$ defined as

$$\kappa_i = \frac{\|v_i\| \|u_i\|}{|\langle v_i, u_i \rangle|}, \quad (2.6)$$

with $\langle \cdot, \cdot \rangle$ the inner product associated with the norm $\|\cdot\|$, u_i the right-eigenvector satisfying $Mu_i = \lambda_i u_i$ and v_i the left-eigenvector satisfying $M^\dagger v_i = \bar{\lambda}_i v_i$. Condition numbers manage to quantify the effect of perturbations of size ε through only the knowledge of the orthogonality between the eigenvectors of the unperturbed operator and its adjoint. Explicitly, for a perturbation V of size ε we have:

$$|\lambda_i(\varepsilon) - \lambda_i| \leq \varepsilon \kappa_i, \quad (2.7)$$

where $\{\lambda_i(\varepsilon)\}$ are the eigenvalues of the perturbed operator $M(\varepsilon) = M + V$ and $\|V\| = \varepsilon$. For normal matrices all eigenvalues are stable and have condition number 1.

2.1 Pseudospectra of rectangular matrices

As we shall see explicitly in section 3, rectangular matrices typically appear when discretizing an eigenvalue problem subject to a constraint. In these cases, pseudoresonances can become important and spectra often fail to give a complete description of the physics. In fact, a rectangular matrix can have an empty spectrum while presenting highly non-trivial dynamics associated with pseudoresonances.

The above discussion of pseudospectra for $N \times N$ square matrices can be easily extended to rectangular matrices (see chapter 8 of [1] for a more detailed discussion). For the sake of generality, let us further assume that these rectangular matrices solve a generalized eigenvalue problem of the form²

$$(M - \lambda_i Q)u_i = 0. \quad (2.8)$$

Then, definitions 2.1-2.3 above hold provided we change $\mathbb{I} \rightarrow Q$ and properly take into account that a matrices $M, Q \in \mathbb{C}^{M \times N}$ ($M \geq N$) are operators from a \mathbb{C}^N vector space with inner product $\langle \cdot, \cdot \rangle_{G_1}$ to a \mathbb{C}^M vector space with inner product

²As we will see in the following sections, we typically do get standard eigenvalue problems when dealing with rectangular matrices. We construct the rectangular problem to be equivalent to a square problem restricted to a subsection of the function space satisfying a given constraint. Hence, the identity matrix is replaced by a matrix that generically differs from the rectangular identity but is equivalent to the restriction of the square identity.

$\langle \cdot, \cdot \rangle_{G_2}$.³ This requires us to generalize the definition of the operator norm (2.5) to

$$\|V\| = \|V\|_{G_1 \rightarrow G_2} = \max_{u \in \mathbb{C}^N} \frac{\|Vu\|_{G_2}}{\|u\|_{G_1}} \quad \text{for } V : \mathbb{C}^N \rightarrow \mathbb{C}^M, \quad (2.9)$$

$$\|W\| = \|W\|_{G_2 \rightarrow G_1} = \max_{u \in \mathbb{C}^M} \frac{\|Wu\|_{G_1}}{\|u\|_{G_2}} \quad \text{for } W : \mathbb{C}^M \rightarrow \mathbb{C}^N, \quad (2.10)$$

and of the resolvent $\mathcal{R}(z; M) : \mathbb{C}^M \rightarrow \mathbb{C}^N$ to

$$\mathcal{R}(z; M) = [(M - zQ)^*(M - zQ)]^{-1} (M - zQ)^* = (M - zQ)^+ \quad (2.11)$$

where we have swapped the usual inverse for the pseudoinverse.

Regarding condition numbers, in order to preserve the physical interpretation of equation (2.7), we have to modify equation (2.6) to the following

$$\kappa_i = \frac{\|v_i\|_{G_2} \|u_i\|_{G_1}}{|\langle v_i, Qu_i \rangle_{G_2}|}, \quad (2.12)$$

with u_i the right-eigenvector satisfying $(M - Q\lambda_i)u_i = 0$ and v_i the left-eigenvector satisfying $(M^\dagger - \bar{\lambda}_i Q^\dagger)v_i = 0$. Here, for an operator $V : \mathbb{C}^N \rightarrow \mathbb{C}^M$, we define the adjoint $V^\dagger : \mathbb{C}^M \rightarrow \mathbb{C}^N$ as a solution to⁴

$$\langle V^\dagger v, u \rangle_{G_1} = \langle v, Vu \rangle_{G_2}, \quad \text{for } v \in \mathbb{C}^M \text{ and } u \in \mathbb{C}^N. \quad (2.13)$$

Note that v_i in equation (2.12) is not unique as $(M^\dagger - \bar{\lambda}_i Q^\dagger)v_i = 0$ is an underdetermined system of equations. This in turn implies that κ_i depends on the particular choice of v_i . Hence, to impose the strictest constraint (2.7), we have to minimize κ_i over all possible solutions v_i . This requires minimization over $M - N - 1$ complex variables and thus is numerically very intensive.

With these modifications in mind, let us collect an important result which will allow us to greatly simplify numerical computations [1]. Given two operators $M, Q \in \mathbb{C}^{N \times M}$ from a \mathbb{C}^N vector space with inner product $\langle \cdot, \cdot \rangle_{G_1}$ to a \mathbb{C}^M ($M \geq N$) vector space with inner product $\langle \cdot, \cdot \rangle_{G_2}$ where

$$\langle v, u \rangle_{G_1} = \sum_{i,j=1}^N \bar{v}^i (G_1)_{ij} u^j, \quad \langle v, u \rangle_{G_2} = \sum_{i,j=1}^M \bar{v}^i (G_2)_{ij} u^j, \quad (2.14)$$

with $G_1 = T^*T$ and $G_2 = F^*F$ symmetric positive definite $N \times N$ and $M \times M$ matrices. The ε -pseudospectrum associated with the eigenvalue problem $(M - \lambda Q)u = 0$ can be computed as

$$\sigma_\varepsilon(M) = \{z \in \mathbb{C} : s_{\min} [F(M - zQ)T^{-1}] > \varepsilon\}. \quad (2.15)$$

³When dealing with generalized eigenvalue problems there are multiple alternative definitions for pseudospectrum (see e.g., chapter 45 of [1] for a discussion). Our choice is consistent with the one presented in [26] which was argued to be the physically-motivated one in the context of pseudospectra.

⁴Note that V^\dagger is only uniquely defined on the image of V . Nonetheless, this ambiguity does not affect condition numbers.

where s_{\min} is defined as

$$s_{\min}(X) = \min \sqrt{\sigma(X^*X)}. \quad (2.16)$$

The condition numbers $\{\kappa_i\}$ of the eigenvalue problem $(M - \lambda Q)u = 0$ are

$$\kappa_i = \frac{\|\tilde{v}_i\|_{2(M)} \|\tilde{u}_i\|_{2(N)}}{|\langle \tilde{v}_i, FQT^{-1}\tilde{u}_i \rangle_{2(M)}|}, \quad (2.17)$$

where $\langle \cdot, \cdot \rangle_{2(L)}$ denotes the usual euclidean inner product in \mathbb{C}^L and \tilde{u}_i and \tilde{v}_i satisfy

$$[F(M - \lambda_i Q)T^{-1}] \tilde{u}_i = 0, \quad [F(M - \lambda_i Q)T^{-1}]^* \tilde{v}_i = 0, \quad (2.18)$$

with \tilde{v}_i chosen to be the solution minimizing κ_i .

2.1.1 An example

In order to illustrate the previous discussion on pseudospectra of rectangular eigenvalue problems, here we consider a simple example. Let us first start by motivating how a rectangular eigenvalue problem might arise from a constrained system. Consider a standard eigenvalue problem

$$Au - \lambda \mathbb{I}u = \begin{pmatrix} 1.50 & 5.40 & 1.78 & -8.42 \\ 0.146 & -1.85 & 0.794 & 3.52 \\ -0.104 & -2.89 & -1.40 & 6.27 \\ -1.10 & -3.69 & -2.03 & 6.04 \end{pmatrix} \begin{pmatrix} u_1 \\ u_2 \\ u_3 \\ u_4 \end{pmatrix} - \lambda \begin{pmatrix} u_1 \\ u_2 \\ u_3 \\ u_4 \end{pmatrix} = 0 \quad (2.19)$$

where the fields are not independent and instead are forced to satisfy the constraint

$$2u_1 + \sqrt{2}u_2 + u_3 + u_4 = 0. \quad (2.20)$$

Hence, formally we would like to find solutions to the eigenvalue problem (2.19) living in the subspace $\mathcal{K} \subset \mathbb{C}^4$ isomorphic to \mathbb{C}^3 , satisfying the constraint (2.20). A straightforward way to do this is to reformulate the problem as a rectangular eigenvalue problem. First, we start by define a rectangular matrix \mathcal{C}

$$\mathcal{C} = \begin{pmatrix} 1 & 0 & 0 \\ 0 & 1 & 0 \\ 0 & 0 & 1 \\ -2 & -\sqrt{2} & -1 \end{pmatrix} \quad (2.21)$$

which embeds vectors in \mathbb{C}^3 into the subspace \mathcal{K} of \mathbb{C}^4 . With this we then proceed to solve the following rectangular eigenvalue problem

$$A\mathcal{C}v - \lambda \mathcal{C}v = \begin{pmatrix} 18.3 & 17.3 & 10.2 \\ -6.9 & -6.8 & -2.7 \\ -12.6 & -11.8 & -7.7 \\ -13.2 & -12.2 & -8.1 \end{pmatrix} \begin{pmatrix} v_1 \\ v_2 \\ v_3 \end{pmatrix} - \lambda \begin{pmatrix} 1 & 0 & 0 \\ 0 & 1 & 0 \\ 0 & 0 & 1 \\ -2 & -\sqrt{2} & -1 \end{pmatrix} \begin{pmatrix} v_1 \\ v_2 \\ v_3 \end{pmatrix} = 0 \quad (2.22)$$

which, by construction is equivalent to (2.19) restricted to \mathcal{K} as \mathcal{C} is a one-to-one map of \mathbb{C}^3 into \mathcal{K} . It is worth mentioning, that for generic rectangular eigenvalue problems, we are not guaranteed to find solutions. Nonetheless in this case we do find two eigenvalues $\lambda = 0$ and $\lambda = 1$.

Now, having identified the rectangular eigenvalue problem, we seek to study the corresponding pseudospectrum. To do so we need to define inner products on \mathbb{C}^3 and \mathbb{C}^4 . For \mathbb{C}^4 we take the standard euclidean inner product $\langle \cdot, \cdot \rangle_4$

$$\langle u_{(1)}, u_{(2)} \rangle_4 = \sum_{i=1}^4 \bar{u}_{(1)}^i u_{(2)}^i, \quad u_{(1)}, u_{(2)} \in \mathbb{C}^4, \quad (2.23)$$

and, for consistency, on \mathbb{C}^3 we take the inner product $\langle \cdot, \cdot \rangle_3$ to be

$$\langle v_{(1)}, v_{(2)} \rangle_3 = \langle \mathcal{C}v_{(1)}, \mathcal{C}v_{(2)} \rangle_4, \quad v_{(1)}, v_{(2)} \in \mathbb{C}^3, \quad (2.24)$$

so that after the embedding we recover the \mathbb{C}^4 inner product of the corresponding states in \mathcal{K} .

Hence, we can now identify the matrices $G_1 = \mathcal{C}^* \mathbb{I}_3 \mathcal{C}$ and $G_2 = \mathbb{I}_3$ we use equations (2.15) and (2.17) to compute the pseudospectrum and the condition numbers. In figure 1 we plot the pseudospectrum. Remarkably, we observe that besides the two eigenvalues $\lambda = 0$ and $\lambda = 1$ there is also a pseudoresonance at $\lambda \sim 2.2$. Furthermore we can see that the restriction of A to \mathcal{K} is spectrally unstable, as small for ε the boundary of the ε -pseudospectra contains both eigenvalues and the pseudoresonance. This instability is further confirmed by the condition numbers which are 9.3 and 24.5 for the eigenvalues $\lambda = 0$ and $\lambda = 1$, respectively. The resolvent of a square matrix is an analytic function in z and its norm obeys a maximum principle: it can take a maximum value only on the boundary of its domain of definition, i.e. the complex plane except for isolated singularities corresponding to the spectrum [1]. Therefore a pseudoresonance can not appear in this case. For rectangular matrices this is no longer true since the resolvent based on the pseudoinverse is not analytic in z and therefore maxima (and minima) can appear in the pseudospectrum as in our simple example. In the following we will compute the pseudospectrum for longitudinal gauge fields in AdS black hole spacetimes. The presence of a constraint in the equations of motion will naturally lead us to a formulation in terms a rectangular eigenvalue problem. This raises the question if pseudoresonances appear in this formulation. It would mean that the formulation in terms of a single masterfield equation leading to a square matrix problem was insufficient to address the pseudospectrum for gauge fields. As we shall see in the following this is not the case. No pseudoresonances appear in the rectangular formulation and indeed the pseudospectra of the approach based directly on the gauge fields and the approach based on a master field agree numerically to high accuracy.

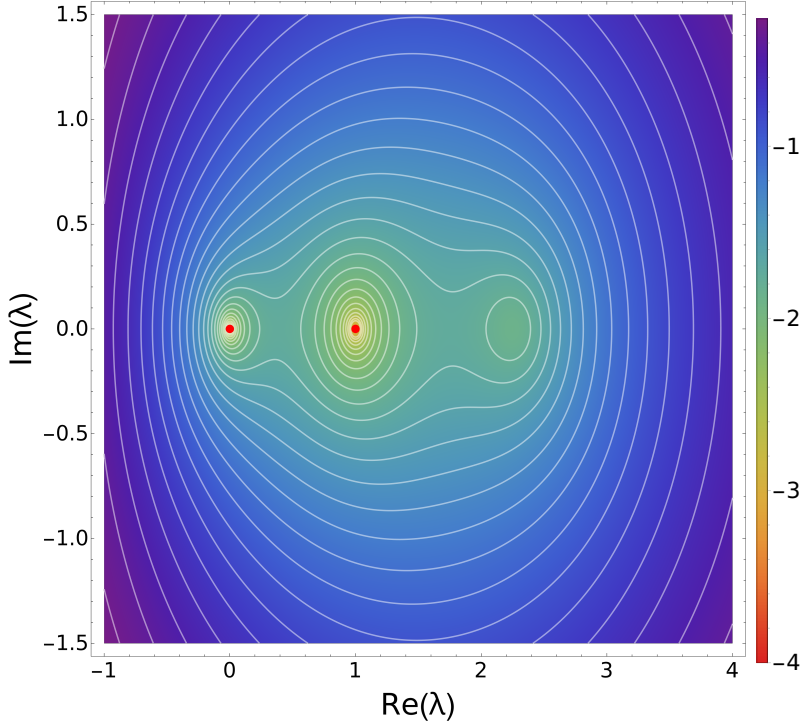


Figure 1: Pseudospectrum of $AC - \lambda C$ in (2.22). The red dots correspond to the eigenvalues, the white lines represent the boundaries of various ε -pseudospectra, and the heat map represent to the logarithm in base 10 of the inverse of the norm of the resolvent.

3 Longitudinal gauge field

Here we focus on the pseudospectra of QNFs and CLMs of the longitudinal sector of U(1) gauge field with action (1.1) in a generic black hole/brane background with metric of the form

$$\begin{aligned} ds^2 &= g_{\mu\nu}(\rho)dx^\mu dx^\nu + R(\rho)^2 ds_{d-1}^2, \\ ds_{d-1}^2 &= \gamma_{ij}(y)dy^i dy^j, \end{aligned} \tag{3.1}$$

This form of the metric is slightly more general than the black brane metrics in (1.2). The functions $g_{\mu\nu}$, R and γ_{ij} can be easily identified for the black brane. We prefer this slightly more general form since in section 6.5 we will briefly consider an AdS₅ black hole with spherical horizon topology. We take $x^\mu \in \{t, \rho\}$ and denote the rest of the coordinates by y^i , $i \in \{1, \dots, d-1\}$.

As we shall see in section 4, one can study pseudospectra for this system introducing a master scalar field. However, in this approach the energy norm is postulated and a priori it is unclear whether it captures the notion of correct energy or if it instead misses features associated with the fundamental structure of the gauge field. For this reason, in this section we propose a new formulation where we work directly

in terms of the gauge field variables. This allows us to avoid introducing new ingredients such as the master scalar and thus ensures we are capturing the right physics. To make our presentation more transparent, we focus on the problem of studying the pseudospectrum of QNFs and we will discuss the necessary modifications for CLMs in the next subsection.

We start by decomposing a $(d + 1)$ -dimensional gauge field according to the isometries of ds_{d-1}^2 as

$$A = A_\mu dx^\mu + \left(\partial_i A^{(L)} + A_i^{(T)} \right) dy^i, \quad (3.2)$$

where $A_i^{(T)}$ satisfies $D^i A_i^{(T)} = 0$ with D the covariant derivative associated with ds_{d-1}^2 . This decomposition makes explicit the existence of two distinct decoupled sectors. The first is the transverse sector, comprised of $A_i^{(T)}$, which is gauge invariant and transforms non-trivially under the isometries of ds_{d-1}^2 . The second is the longitudinal sector, comprised of $\{A_\mu, A^{(L)}\}$ which behaves as a scalar under the isometries of ds_{d-1}^2 and transforms under gauge transformations in the following way

$$A_\mu \rightarrow A_\mu + \partial_\mu \chi, \quad A^{(L)} \rightarrow A^{(L)} + \chi. \quad (3.3)$$

From this point forward, we focus solely on the longitudinal sector and we completely remove the gauge freedom by fixing gauge to $A^{(L)} = 0$.

We expand the gauge field components in eigenfunctions of the ds_{d-1}^2 Laplacian \square_{d-1}

$$A_\mu = \sum_{\lambda^2, m} A_\mu^{(\lambda^2, m)} Y_{(\lambda^2, m)} \quad \text{with} \quad \square_{d-1} Y_{(\lambda^2, m)} = -\lambda^2 Y_{(\lambda^2, m)}. \quad (3.4)$$

where here m is a multi-index resolving the degeneracy of λ^2 and the set $\{Y_{(\lambda^2, m)}\}$ is a complete basis of \square_{d-1} .⁵ Sectors with different λ^2 decouple and we can treat them independently. Henceforth, unless explicit spacetime dependence on y^i is given, we always assume that the above decomposition has been performed and we drop the (λ^2, m) superindex.

With this, in gauge $A_L = 0$ and focusing on the sector with eigenvalue $-\lambda^2$ of the ds_{d-1}^2 Laplacian, we find that the Maxwell equations $\nabla_M F^{MN} = 0$ can be written schematically an eigenvalue problem for the operator $i\partial_t$ plus a constraint

⁵For a spherical black hole, λ^2 is the total angular momentum and m labels the angular momenta of the smaller spheres forming the S^{d-1} . For a planar black hole λ^2 is the total linear momentum along the plane and m labels the direction of the momentum. In this case the sum has to be exchanged by an integral.

independent of $i\partial_t$

$$\begin{aligned} i\partial_t\Phi = \omega\Phi &= i \begin{pmatrix} \lambda^2 \frac{g}{R^2} (g^{t\rho} A_t + g^{\rho\rho} A_\rho) \\ (\alpha_\rho + \partial_\rho A_t) \\ -\frac{1}{g^{tt}} \left[g^{t\rho} (\alpha_\rho + \partial_\rho A_t) + \frac{R^{3-d}}{\sqrt{-g}} \partial_\rho \left\{ \sqrt{-g} R^{d-3} (g^{t\rho} A_t + g^{\rho\rho} A_\rho) \right\} \right] \end{pmatrix} \\ &= \begin{pmatrix} \mathcal{L}_{11} & \mathcal{L}_{12} & \mathcal{L}_{13} \\ \mathcal{L}_{21} & \mathcal{L}_{22} & \mathcal{L}_{23} \\ \mathcal{L}_{31} & \mathcal{L}_{32} & \mathcal{L}_{33} \end{pmatrix} \begin{pmatrix} \alpha_\rho \\ A_\rho \\ A_t \end{pmatrix} = \mathcal{L}\Phi, \end{aligned} \quad (3.5)$$

$$\mathcal{L}_0\Phi = \frac{1}{\sqrt{-g}R^{d-1}} \partial_\rho \left(\frac{R^{d-1}}{\sqrt{-g}} \alpha_\rho \right) - \frac{\lambda^2}{R^2} (g^{tt} A_t + g^{t\rho} A_\rho) = 0, \quad (3.6)$$

with $g = \det\{g_{\mu\nu}\}$, $\Psi = (\alpha_\rho, A_\rho, A_t)^T$, $\alpha_\rho = \partial_t A_\rho - \partial_\rho A_t$ an auxiliary variable introduced to make the problem linear in ∂_t and ω the QNF. Although we have more equations than fields, the system itself is not overdetermined as the equations are related by the off-shell identity $\nabla_N \nabla_M F^{MN} = 0$. Hence, naively one could try to forget the constraint and solve the eigenvalue problem (3.5). This leads however to unphysical modes appearing at $\omega = 0$ associated with the fact that any solution $\mathcal{L}_C\Phi = c$ with c a constant, fulfills the off-shell identity and the eigenvalue problem (3.5) despite failing to satisfy the constraint (3.6). Alternatively, we might try to work with a singular eigenvalue problem resulting from replacing a row in $(\mathcal{L} - \omega)\Phi$ by $\mathcal{L}_0\Phi$. However, this choice would complicate the physical interpretation as we would have to deal with a generalized eigenvalue problem (see appendix A for a discussion) and can even lead to the appearance of spurious modes associated with the singular character of the problem which again would spoil the pseudospectrum making it difficult to discern physical from unphysical artifacts. Lastly, we could use (3.6) to remove one of the gauge field variables (e.g. A_t) and build a standard eigenvalue problem for the remaining two by ignoring one of the equations in (3.5). By construction, this new eigenvalue problem would be free from the previously discussed unphysical modes and thus could be used to study the pseudospectra of QNFs. However, this approach requires us to be able to solve analytically the constraint, which need not be possible in more complicated settings. In fact, for the CLMs this is indeed not possible as in the constraint all the fields entering appear together with their derivatives. Moreover, from the perspective of being as fundamental as possible, this simplified approach seems potentially dangerous as it is using an on-shell equation and ignoring another, which suggests that we might be leaving out some bounded perturbations in our study of the pseudospectra.

In conclusion, to avoid making any assumptions that could restrict the perturbations allowed in pseudospectra, we would like to solve both the eigenvalue problem (3.5) and the constraint equation (3.6) simultaneously without ignoring any of the equations. That is, we want to solve the eigenvalue problem (3.5) restricted to a subspace of the function space where Φ satisfies the constraint (3.6). Generically let

us write

$$\Phi = \begin{pmatrix} \alpha_\rho \\ A_\rho \\ A_t \end{pmatrix} = \begin{pmatrix} 1 & 0 \\ 0 & 1 \\ \mathcal{C}_1 & \mathcal{C}_2 \end{pmatrix} \begin{pmatrix} \alpha_\rho \\ A_\rho \end{pmatrix} = \mathcal{C}\Psi \quad (3.7)$$

with \mathcal{C}_1 and \mathcal{C}_2 operators resulting from solving for A_t in (3.6).⁶ We can then study the following (generalized) rectangular eigenvalue problem

$$\mathcal{L}_\mathcal{C} - \omega \mathcal{I}_\mathcal{C} = (\mathcal{L} - \omega \mathcal{I})\mathcal{C}, \quad (3.8)$$

and its pseudospectrum (here \mathcal{I} is the identity operator). This is equivalent to studying the spectrum and pseudospectrum of the restriction of \mathcal{L} defined in (3.5) to the relevant subspace \mathcal{K} of the function space \mathcal{H} comprised of functions satisfying the constraint (3.6).⁷ The eigenvalue problem for $\mathcal{L}_\mathcal{C} : \mathcal{K} \rightarrow \mathcal{H}$ is thus rectangular and, after discretization in a grid, the pseudospectrum can be studied according to our discussion in section 2.1.

Regarding the norms, we take the usual prescription and define the physically motivated norm from the energy. The energy momentum tensor of the gauge field is

$$T_{MN} = F_{MS}F_N{}^S - \frac{1}{4}g_{MN}F_{SP}F^{SP}, \quad (3.9)$$

and leads to the following expression for the energy norm

$$E[A] = \int d\rho \sqrt{-g} R^{d-1} \left\{ \frac{1}{|g|} |\partial_t A_\rho - \partial_\rho A_t|^2 + \frac{\lambda^2}{R^2} (g^{\rho\rho} |A_\rho|^2 + |g^{tt}| |A_t|^2) \right\}, \quad (3.10)$$

where we have dropped the sum over the different eigenvalues $\{\lambda\}$ of the Laplacian of ds_{d-1}^2 as we in a sector with fixed λ . With this, introducing an auxiliary field α_ρ defined in equation (3.6), the final expression for the inner product is given by

$$\langle \Phi^{(1)}, \Phi^{(2)} \rangle_E = \int \sqrt{-g} R^{d-1} \left\{ \frac{1}{|g|} \bar{\alpha}_\rho^{(1)} \alpha_\rho^{(2)} + \frac{\lambda^2}{R^2} (g^{\rho\rho} \bar{A}_\rho^{(1)} A_\rho^{(2)} + |g^{tt}| \bar{A}_t^{(1)} A_t^{(2)}) \right\}, \quad (3.11)$$

In a bit more detail, we take this inner product to be the inner product defining \mathcal{H} , the space of functions Φ with finite energy. This is consistent with the usual approach for standard eigenvalue problems and allows for an adequate identification of the convergence bands of the QNF pseudospectrum [76]. The inner product on \mathcal{K} is given by the projection of the inner product on \mathcal{H} to the subspace \mathcal{K}

$$\langle \Psi^{(1)}, \Psi^{(2)} \rangle_E = \langle \mathcal{C}\Psi^{(1)}, \mathcal{C}\Psi^{(2)} \rangle_E, \quad \text{for } \Psi^{(1)}, \Psi^{(2)} \in \mathcal{K}. \quad (3.12)$$

⁶The constraint equation can be solved numerically in a grid to obtain a discretized version of \mathcal{C} directly.

⁷By construction \mathcal{C} uplifts $\Psi = (\alpha_\rho, A_\rho)^T$ to a function Φ in \mathcal{H} satisfying the constraint (3.6). Hence we abuse notation and use \mathcal{K} to denote both the domain of $\mathcal{L}_\mathcal{P}$ comprised of functions Ψ , as well as its uplift to functions $\Phi = \mathcal{C}\Psi$.

We finish this section by discussing the domain of convergence of the pseudospectra [27, 39, 76]. The lack of convergence of the pseudospectrum is related to the failure of the energy norm to properly impose infalling boundary conditions in the continuum limit. The analytic continuation of outgoing solutions deep into the lower half plane have finite energy and contribute to the pseudospectrum based on the energy norm. Let us assume that near the event horizon $\rho = 0$ the metric takes the following form

$$ds^2 = (-4\pi T\rho dt^2 + 2dtd\rho + 2d\rho^2) + s_{\text{BH}} ds_{d-1}^2 \quad (3.13)$$

with s_{BH} and T , the entropy density and temperature of the black hole/brane, respectively. Then, from the near horizon behavior of $\langle \mathcal{L}_C \Psi^{(1)}, \mathcal{L}_C \Psi^{(1)} \rangle$ it follows that modes with an outgoing component $\Psi^{(1)} \sim \rho^{-i\omega/(2\pi T)}$ yield a finite norm if $\text{Im}(\omega) < -\pi T$. Hence, the domain of \mathcal{L}_C contains modes with $\text{Im}(\omega) < -\pi T$ that have finite energy but are not infalling. Thus in the continuum limit the spectrum of \mathcal{L}_C is comprised of the QNFs with $\text{Im}(\omega) > -\pi T$ together with the continuum $\text{Im}(\omega) < -\pi T$. Hence, the pseudospectrum computed numerically in a grid only converges for $\text{Im}(\omega) > -\pi T$. We comment on the physical implications of this lack of convergence in section 6.2.3 and we explicitly check the prediction for the band of convergence in appendix D.

3.1 Modifications for CLMs

To extend the approach described above to CLMs of black branes we only have to make a few modifications. Firstly, we write the ds_{d-1}^2 portion of the metric in (3.1) as

$$ds_{d-1}^2 = dy_1^2 + d\mathbf{y}_\perp^2, \quad (3.14)$$

and we use the rotational symmetry of \mathbb{R}^{d-1} to fix the momentum \mathbf{k} along y_1 ; i.e., we consider fluctuations depending only on $\{t, \rho, y_1\}$. Now, keeping in mind that for CLMs we want to fix the frequency ω and study $k(\omega)$, we choose the following ansatz for the gauge field

$$A = A_t(t, \rho, y_1) dt + A_\rho(t, \rho, y_1) d\rho + A_1(t, \rho, y_1) dy_1, \quad (3.15)$$

and we expand the time dependence in Fourier modes $e^{-i\omega t}$. As before, we have to deal with the gauge symmetry which for this ansatz reads

$$A_t \rightarrow A_t + \partial_t \chi, \quad A_\rho \rightarrow A_\rho + \partial_\rho \chi, \quad A_1 \rightarrow A_1 + \partial_1 \chi. \quad (3.16)$$

In this case, we remove gauge redundancy by taking $A_t = 0$ gauge.

With all this we conclude that, similar to the situation for QNFs, we can write the Maxwell equations as an eigenvalue problem for $-i\partial_1$ plus a constraint restricting

the function space

$$\begin{aligned}
-i\partial_1\Phi = k\Phi &= -i \begin{pmatrix} R^2 \left[i\omega g^{t\rho} \frac{\sqrt{-g}}{R^{d-1}} \partial_\rho \left(\frac{R^{d-1}}{\sqrt{-g}} A_\rho \right) + \omega^2 g^{tt} A_\rho \right] \\ R^2 \left[\alpha_\rho + \partial_\rho A_1 \right] \\ R^2 \left[-g^{\rho\rho} \frac{\sqrt{-g}}{R^{d-1}} \partial_\rho \left(\frac{R^{d-1}}{\sqrt{-g}} A_\rho \right) + i\omega g^{t\rho} A_\rho \right] \end{pmatrix} \\
&= \begin{pmatrix} \mathcal{L}_{11} & \mathcal{L}_{12} & \mathcal{L}_{13} \\ \mathcal{L}_{21} & \mathcal{L}_{22} & \mathcal{L}_{23} \\ \mathcal{L}_{31} & \mathcal{L}_{32} & \mathcal{L}_{33} \end{pmatrix} \begin{pmatrix} \alpha_\rho \\ A_\rho \\ A_1 \end{pmatrix} = \mathcal{L}\Phi, \tag{3.17}
\end{aligned}$$

$$\begin{aligned}
\mathcal{L}_0\Phi &= -i\omega \frac{g^{t\rho}}{R^2} \alpha_\rho + \frac{1}{\sqrt{-g}R^{d-1}} \partial_\rho \left(R^{d-3} \sqrt{-g} g^{\rho\rho} \alpha_\rho \right) \\
&\quad + \omega^2 \frac{g^{tt}}{R^2} A_1 + \frac{i\omega}{\sqrt{-g}R^{d-1}} \partial_\rho \left(R^{d-3} \sqrt{-g} g^{t\rho} A_1 \right) = 0, \tag{3.18}
\end{aligned}$$

where here $\Phi = (\alpha_\rho, A_\rho, A_1)$ and $\alpha_\rho = \partial_1 A_\rho - \partial_\rho A_1$. As before, we implement the constraint through an uplift \mathcal{C}

$$\Phi = \begin{pmatrix} \alpha_\rho \\ A_\rho \\ A_1 \end{pmatrix} = \begin{pmatrix} 1 & 0 \\ 0 & 1 \\ \mathcal{C}_1 & \mathcal{C}_2 \end{pmatrix} \begin{pmatrix} \alpha_\rho \\ A_\rho \\ A_1 \end{pmatrix} = \mathcal{C}\Psi, \tag{3.19}$$

and instead study spectra and pseudospectra for the rectangular problem $(\mathcal{L} - k\mathcal{I})\mathcal{C}$.

With regards to the norm, we follow [39] and take the energy norm as the time-average of the energy density along the y^1 direction. Thus we take the following prescription for the inner product in $A_t = 0$ gauge

$$\langle \Phi^{(1)}, \Phi^{(2)} \rangle_E = \int d\rho \sqrt{-g} R^{d-1} \left\{ \frac{\omega^2}{|g|} \bar{A}_\rho^{(1)} A_\rho^{(2)} + \frac{1}{R^2} \left(g^{\rho\rho} \bar{\alpha}_\rho^{(1)} \alpha_\rho^{(2)} + |g^{tt}| \omega^2 \bar{A}_1^{(1)} A_1^{(2)} \right) \right\}. \tag{3.20}$$

As we shall see explicitly this inner product does capture the relevant physical notion of size as it reproduces an increasing stability for the gapped CLMs as $\omega \rightarrow 0$.

Lastly we note that as for the master scalar, the fact that we are fixing $\text{Im}(\omega) = 0$ implies that the CLM pseudospectrum will be convergent. Let us see this explicitly following the same approach as we did to identify the convergent region of the QNF pseudospectrum. We assume that near the event horizon $\rho = 0$ the metric takes the form

$$ds^2 = (-4\pi T\rho dt^2 + 2dt d\rho + 2d\rho^2) + s_{\text{BH}} ds_{d-1}^2 \tag{3.21}$$

where s_{BH} and T are the entropy density and the temperature of the black hole/brane, respectively. Then, from the near horizon behavior of $\langle \mathcal{L}_C \Psi^{(1)}, \mathcal{L}_C \Psi^{(1)} \rangle$ it follows that modes with an outgoing component $\Psi^{(1)} \sim \rho^{-i\omega/(2\pi T)}$ yield a finite norm if $\text{Im}(\omega) < -\pi T$. Hence, as we are working in the line $\text{Im}(\omega) = 0$, we are guaranteed that only infalling modes have finite energy. Thus the convergence problems present for the QNFs are absent when dealing with CLMs [39]. The convergence properties of CLM pseudospectra are explicitly checked in appendix D.

4 Master scalar

The master field approach provides a systematic method to address the complexities associated with gauge redundancy. This framework expresses the $d + 1$ components of the gauge vector in terms of $d - 1$ independent, gauge-invariant degrees of freedom (see e.g. [80] for a review). In the case of a U(1) gauge field, this is achieved via the standard longitudinal and transverse decomposition described in section 3. Instead of imposing the gauge condition $A^{(L)} = 0$, we work with gauge-invariant combinations

$$a_\mu = A_\mu - \partial_\mu A^{(L)}. \quad (4.1)$$

Beginning with the Maxwell action (1.1), the fields are expanded in a basis of eigenfunctions of the $(d - 1)$ -dimensional Laplacian (3.4). Integrating over the transverse directions produces an effective two-dimensional action for each longitudinal mode

$$S^{(L)}[a] = - \int d^2x \sqrt{-g} \left\{ R^{d-1} g^{\mu\nu} \partial_\alpha \bar{a}_\mu \partial^\alpha a_\nu + \lambda^2 R^{d-3} g^{\mu\nu} \bar{a}_\mu a_\nu \right\}. \quad (4.2)$$

For notational simplicity, we have suppressed the mode labels (λ^2, m) . The two-dimensional field a is massive and propagates one degree of freedom. To isolate this degree of freedom, we introduce an auxiliary scalar field ψ through the interaction term

$$S_c[\psi, a] = - \int d^2x \sqrt{-g} \left\{ R^{-2} \left| \lambda \psi + R^{(d-1)/2} \epsilon^{\mu\nu} \nabla_\mu a_\nu \right|^2 \right\}. \quad (4.3)$$

This term is chosen to cancel the kinetic term of $S^{(L)}[a]$. When the scalar ψ is on shell, $S_c[\psi[a], a] = 0$ for any a . These choices allow us to find an exact solution for a in the coupled system

$$\delta_a (S^{(L)}[a] + S_c[\psi, a]) = 0 \quad \rightarrow \quad a[\psi]_\mu = \frac{1}{\lambda R^{d-3}} \epsilon_{\mu\nu} \nabla^\nu (R^{(d-3)/2} \psi). \quad (4.4)$$

Substituting this relation back into the action yields a theory formulated solely in terms of the master scalar.

$$\begin{aligned} S^{(L)}[a] + S_c[\psi, a] &= S[\psi] = - \int d^2x \sqrt{-g} \left\{ |\partial\psi|^2 + V(\phi, R) |\psi|^2 \right\}, \\ V &= \frac{\lambda^2}{R^2} + \frac{(d-3)}{2} \left(\square \log(R) + \frac{(d-3)}{2} \nabla_\mu \log(R) \nabla^\mu \log(R) \right). \end{aligned} \quad (4.5)$$

So for any ψ_{OS} extremizing (4.5), using (4.4), we can obtain a solution for the longitudinal mode. Using the auxiliary field $\phi = \partial_t \psi$ we can write the EoMs as an eigenvalue problem

$$\begin{aligned} i\partial_t \begin{pmatrix} \phi \\ \psi \end{pmatrix} &= \omega \begin{pmatrix} \phi \\ \psi \end{pmatrix} = i \begin{pmatrix} \mathcal{L}^{(1)} & \mathcal{L}^{(2)} \\ 1 & 0 \end{pmatrix} \begin{pmatrix} \phi \\ \psi \end{pmatrix}, \\ \mathcal{L}^{(1)}\phi &= -g^{tt} (\partial_\rho g_{t\rho} \phi + 2g_{t\rho} \partial_\rho \phi), \\ \mathcal{L}^{(2)}\psi &= -g^{tt} [\partial_\rho (g_{tt} \partial_\rho \psi) + V\psi]. \end{aligned} \quad (4.6)$$

4.1 Boundary Conditions

In the analysis of Quasinormal Modes, it is essential to consider not only the equations of motion but also the associated boundary conditions. Assuming we start from a gauge field on an AdS background, the potential can be expanded at large distances (large R), corresponding to the vicinity of the AdS boundary. Solving the equations of motion for the master scalar in this regime yields two solutions

$$\psi = \psi_{\pm} R^{\Delta_{\pm}}, \quad \Delta_{\pm} = -\frac{1}{2} \pm \frac{d-4}{2}, \quad (4.7)$$

Substituting this expansion into (4.4) clarifies the correspondence: ψ_+ represents the source of the gauge field, whereas ψ_- denotes the expectation value (vev) of the QFT operator dual to the gauge field. On spaces with dimension five or greater, fixing the source of the gauge field corresponds to fixing the leading mode of the scalar (standard quantisation). For spaces with fewer than five dimensions, one should fix the subleading mode of the scalar (alternate quantisation [81]).

4.2 Energy Norm

We will use the energy norm to compute the pseudo-spectra for the eigenvalue problem of the master scalar. There are two distinct methods for computing the energy. The standard approach involves calculating the energy directly from (4.5), under the assumption that V is independent of the metric, resulting in

$$E[\psi] = \int d\rho \sqrt{-g} \left(-g^{tt} |\partial_t \psi|^2 + g^{\rho\rho} |\partial_\rho \psi|^2 + V |\psi|^2 \right). \quad (4.8)$$

Alternatively, we can compute the energy from the original action (1.1) and use the transformation (4.4), yielding

$$E[a[\psi]] = \int d\rho \sqrt{-g} \left(-g^{tt} |\partial_t \psi|^2 + \frac{g^{\rho\rho}}{R^{d-3}} |\partial_\rho R^{(d-3)/2} \psi|^2 + \frac{\lambda^2}{R^2} |\psi|^2 \right). \quad (4.9)$$

Generally, these two approaches differ by a boundary term. In asymptotically AdS spacetimes, the boundary term contributes only at the conformal boundary.

$$E[a[\psi]] = E[\psi] + \frac{d-3}{2L^2} \left| \sqrt{R} \psi \right|^2 \Big|_{\partial \text{AdS}}, \quad (4.10)$$

Substituting the asymptotic expansion from (4.7) and setting the gauge field source to zero reveals that the boundary term contributes only in three and five dimensions, thereby shifting the positive definiteness of $E[\psi]$

$$E[\psi] \geq \int d\rho \sqrt{-g} \left(\frac{\lambda^2}{R^2} |\psi|^2 \right) - \frac{d-3}{2L^2} \left| \sqrt{R} \psi \right|^2 \Big|_{\partial \text{AdS}}. \quad (4.11)$$

One can check that for any 5-dimensional, asymptotically AdS Black Hole the field $\psi = \psi_0 R^{-1/2}$ obeys the right boundary conditions and exactly saturates the bound (4.11). Therefore, the norm (4.8) is not positive definite for $\lambda^2 < (R_h/L)^2$ where R_h is the radius of the horizon. Instead, using (4.9) as the norm for the inner product, we ensure there are no negative-norm states.⁸ The following definition is establishes the inner product

$$\langle \Phi^{(1)}, \Phi^{(2)} \rangle = \int d\rho \sqrt{-g} \left(\frac{g^{\rho\rho}}{R^{D-4}} (\partial_\rho R^{(d-3)/2}) \bar{\psi}^{(1)} (\partial_\rho R^{(d-3)/2}) \psi^{(2)} \right. \\ \left. - g^{tt} \bar{\phi}^{(1)} \phi^{(2)} + \frac{\lambda^2}{R^2} \bar{\psi}^{(1)} \psi^{(2)} \right). \quad (4.12)$$

Following the same approach as in section 3, we find that the convergence properties match those found in that section.

5 Hodge duality

The master scalar presents a way to compute the QNMs of a gauge field in terms of a 2-dimensional scalar field. However, as we are reducing to 2 dimensions, this approach does not allow us to pose the problem of computing CLMs. In order to consider that problem, let us reduce the gauge field to a 3-dimensional space where we include one flat coordinate y_1 . In this section we will focus on the black brane case, that is where $\gamma_{ij} = \delta_{ij}$. We are relabeling the coordinates $x^\mu = \{t, \rho, y_1\}$ and y^i denote the rest of coordinates on the plane \mathbb{R}^{d-1} different from y_1 . With these modifications, we consider the full metric (3.1) and gauge field of the form of section 3.1:

$$ds^2 = \tilde{h}_{\mu\nu} dx^\mu dx^\nu + R^2 ds_{d-2}^2, \\ A = A_\mu(x^\mu) dx^\mu. \quad (5.1)$$

Using this ansatz on (1.1), after an integration of the transverse space, we find the following 3-dimensional problem. For one mode:

$$S^{(L)}[A] = -\frac{1}{4} \int d^3x \sqrt{-\tilde{h}} R^{d-2} F_{(3)}^2. \quad (5.2)$$

To transform this expression into the canonically normalized Maxwell action we may rescale the 3-dimensional metric as $h_{\mu\nu} = R^{-2(d-2)} \tilde{h}_{\mu\nu}$. In that metric the action reads:

$$S^{(L)}[A] = -\frac{1}{4} \int d^3x \sqrt{-h} F_{(3)}^2. \quad (5.3)$$

⁸We note that in [26] the authors use the non-positive norm (4.8). The presence of negative eigenvalues in the norm can be addressed numerically by applying appropriate techniques. While this can in principle be done, our approach circumvents these subtleties altogether.

We may notice that, under the symmetry assumptions we have taken, the problem of a $(d + 1)$ -dimensional gauge field gets reduced to study a 3-dimensional gauge field. A 3D gauge field carries one single degree of freedom, which we can extract by performing the following change:

$$F_{\mu\nu} = \epsilon_{\mu\nu\sigma} \partial^\sigma \psi_*, \quad (5.4)$$

where ψ_* is a scalar field. This change can be understood as Hodge duality, written in form language $F = \star d\psi_*$. This relation is manifesting explicitly the counting of degrees of freedom of a 3-dimensional gauge field, being then dual to a massless scalar field. Since in this way we introduce a scalar that is off-shell equivalent to the degrees of freedom of the gauge field in 3-dimensions, we should expect that the pseudospectra of the gauge field and the master field coincide. Plugging this in the action, we finally arrive to:

$$S^{(L)}[A] = S[\psi_*] = \frac{1}{2} \int d^3x \sqrt{-h} (\partial\psi_*)^2. \quad (5.5)$$

We are interested in comparing this with the master scalar introduced in Section 4. By taking $\mu = y_1$ in equation (5.4) we arrive to:

$$(k_1 A_\nu - \partial_\nu A_1) = \epsilon_{1\nu\sigma} \partial^\sigma \psi_*. \quad (5.6)$$

As we are reducing to a 2-dimensional scalar, we may set $A_1 = 0$. Then, by defining $\epsilon_{\mu\nu 1} = R^{3-d} \epsilon_{\mu\nu}^{(2)}$:

$$A_\nu = \frac{1}{k_1 R^{d-3}} \epsilon_{\nu\sigma}^{(2)} \partial^\sigma \psi_* \quad (5.7)$$

where now greek indices run over $\nu = \{t, \rho\}$. Comparing with (4.4), we define $\psi_* = R^{(d-3)/2} \psi$, arriving to

$$A_\mu = \frac{1}{k_1 R^{d-3}} \epsilon_{\mu\nu}^{(2)} \nabla^\nu (R^{(d-3)/2} \psi). \quad (5.8)$$

Finally, we may notice that this relation is invariant under 2-dimensional rescalings of the 2-dimensional metric. Thus, we might scale the 2d metric back to recover exactly (4.4).

The energy-momentum tensor of this 3-dimensional scalar field is given by:

$$T_{\mu\nu} = \partial_\mu \psi_* \partial_\nu \psi_* + \partial_\nu \psi_* \partial_\mu \psi_* - h_{\mu\nu} (\partial\psi_*)^2, \quad (5.9)$$

that gives the following expression for the energy norm:

$$E[\psi_*] = \int d\rho \sqrt{-h} (-h^{tt} |\partial_t \psi_*|^2 + h^{\rho\rho} |\partial_\rho \psi_*|^2 + h^{11} k_1^2 |\psi_*|^2). \quad (5.10)$$

where we have expanded the field in Fourier modes in y_1 . To connect with the master scalar approach, we may express the energy norm using the relation between the two

scalars and recovering the original metric. In terms of the 2-dimensional section of the metric, that norm reads:

$$E[\psi_\star[\psi]] = \int d\rho \sqrt{-g} \left(-g^{tt} |\partial_t \psi|^2 + g^{\rho\rho} \frac{1}{R^{d-3}} |\partial_\rho (R^{(d-3)/2} \psi)|^2 + \frac{k_1^2}{R^2} |\psi|^2 \right), \quad (5.11)$$

so we recover the energy norm (4.10). By recovering the master scalar approach from the reduction to a 3-dimensional Hodge dual scalar, we may notice that we recover in a natural way the well-defined norm for the pseudospectrum problem. We infer from this result that Hodge duality presents an honest way of building a master scalar, thus connecting it to the rectangular matrix pseudospectrum of gauge fields.

5.1 CLMs from Hodge duality

The Hodge dual scalar approach presents a natural way for computing CLMs for a gauge field. The equations of motion of the scalar (5.5) are

$$\square \psi_\star = \frac{1}{\sqrt{-h}} \partial_\mu \left(\sqrt{-h} h^{\mu\nu} \partial_\nu \psi_\star \right) = 0. \quad (5.12)$$

By considering the time dependence $\psi_\star(t, \rho, y_1) = e^{-i\omega t} \psi_\star(\rho, y_1)$ and introducing an auxiliary field $\tilde{\phi}_\star = \partial_1 \psi_\star$, as argued in [39], we can define a well-motivated energy norm starting from the time-averaged energy density along a surface of constant t and y_1 . In our case:

$$\bar{\varrho}[\psi_\star] = \int d\rho \sqrt{-h} \left(-h^{tt} \omega^2 |\psi_\star|^2 + h^{\rho\rho} |\partial_\rho \psi_\star|^2 + h^{11} |\partial_1 \psi_\star|^2 \right). \quad (5.13)$$

Based on this expression we define then the inner product for $\tilde{\Phi}_\star = (\tilde{\phi}_\star, \psi_\star)$:

$$\langle \tilde{\Phi}_\star^{(1)}, \tilde{\Phi}_\star^{(2)} \rangle_E = \int d\rho \sqrt{-h} \left(-h^{tt} \omega^2 \bar{\psi}_\star^{(1)} \psi_\star^{(2)} + h^{\rho\rho} \partial_\rho \bar{\psi}_\star^{(1)} \partial_\rho \psi_\star^{(2)} + h^{11} \bar{\tilde{\phi}}_\star^{(1)} \tilde{\phi}_\star^{(2)} \right). \quad (5.14)$$

We can rewrite this inner product in terms of the 2-dimensional scalar, by using again the relation $\psi_\star = R^{(d-3)/2} \psi$ and the 2-dimensional metric

$$\begin{aligned} \langle \tilde{\Phi}^{(1)}, \tilde{\Phi}^{(2)} \rangle_E = \int d\rho \sqrt{-g} & \left(\frac{g^{\rho\rho}}{R^{d-3}} (\partial_\rho R^{(d-3)/2} \bar{\psi}^{(1)}) (\partial_\rho R^{(d-3)/2} \psi^{(2)}) \right. \\ & \left. - g^{tt} \omega^2 \bar{\psi}^{(1)} \psi^{(2)} + \frac{1}{R^2} \bar{\tilde{\phi}}^{(1)} \tilde{\phi}^{(2)} \right). \end{aligned} \quad (5.15)$$

Finally, in terms of the 2-dimensional scalar, the equation of motion (5.12) can be recasted as an eigenvalue problem:

$$\begin{aligned} -i\partial_1 \begin{pmatrix} \tilde{\phi} \\ \psi \end{pmatrix} &= k_1 \begin{pmatrix} \tilde{\phi} \\ \psi \end{pmatrix} = -i \begin{pmatrix} 0 & \mathcal{L} \\ 1 & 0 \end{pmatrix} \begin{pmatrix} \tilde{\phi} \\ \psi \end{pmatrix}, \\ \mathcal{L}\psi &= R^2 \left[\omega^2 g^{tt} \psi + i\omega \left(2 \frac{g^{t\rho}}{R^{(d-3)/2}} \partial_\rho (R^{(d-3)/2} \psi) + \frac{R^{d-3}}{\sqrt{-g}} \partial_\rho (R^{-(d-3)} \sqrt{-g} g^{\rho t}) \psi \right) \right. \\ &\quad \left. - \frac{R^{(d-3)/2}}{\sqrt{-g}} \partial_\rho (R^{-(d-3)} \sqrt{-g} g^{\rho\rho} \partial_\rho (R^{(d-3)/2} \psi)) \right]. \end{aligned} \quad (5.16)$$

Following the same approach as in section 3.1, we find that the convergence properties match those found in that section.

6 Holographic setup

Having presented both our novel formulation in terms of the gauge field (GF) as well as the standard approach based on the master scalar (MS) we now present and compare pseudospectra in both frameworks for the following scenarios: CLMs and QNFs of a Schwarzschild black brane in AdS_{5+1} , CLMs and QNFs of a Schwarzschild black brane in AdS_{4+1} and QNFs of a Schwarzschild black hole in AdS_{4+1} . We take this choice of spacetimes to illustrate importance of choosing the right energy norm for the MS approach. While in AdS_{5+1} the boundary term in (4.10) plays no role, in AdS_{4+1} the energy norm (4.8) is not positive definite and instead we must use the energy norm (4.9). Naively, one would expect that MS and GF formulations should yield dramatically different pseudospectra. However, we find the same pseudospectra in both frameworks. This agreement can be understood from Hodge duality. As we argued in section 5, the d -dimensional Maxwell action is equivalent to a 3-dimensional Maxwell action in an effective spacetime. The existence of Hodge duality in this reduced spacetime then implies that the gauge field dynamics should be correctly captured by a 3-dimensional scalar field; which can be related to the master scalar. Hence, it follows that MS and GF formulations should coincide.

6.1 CLMs of SAdS_{5+1} black brane

In this subsection we study the CLMs of the longitudinal sector of a gauge field with action (1.1) in a $(5+1)$ -dimensional black brane with metric (1.2) with $d = 5$. Recall that we are working in units where the temperature is fixed to $T = 5/(4\pi)$.

We start by stating the boundary conditions taken in GF and MS frameworks; thus defining the functional spaces under consideration. After that we present and discuss our results showcasing that indeed we find an equivalence between MS and GF approaches.

6.1.1 Boundary conditions in the GF framework

In the GF framework we study the pseudospectra of the eigenvalue problem (3.17) subject to the constraint (3.18) with respect to the inner product (3.20).

In order to properly set up this problem we need to define the functional space by specifying boundary conditions for the gauge field components $\{A_\rho, \alpha_\rho, A_1\}$. To do so, we follow AdS/CFT as our guideline. To have CLMs we impose regularity on the event horizon to select infalling modes and on the AdS boundary we demand that there is no source from the point of view of the dual QFT. To assess this latter point, we solve the equations of motion in the $\rho \rightarrow 1$ region for modes with momentum k

and frequency ω and find the following asymptotic behavior of the fields depending only on two parameters $\{s, v\}$

$$A_\rho = -iks(1 - \rho) + \frac{3ikv}{k^2 - \omega^2}(1 - \rho)^2 + \dots, \quad (6.1a)$$

$$\alpha_\rho = \omega^2 s(1 - \rho) - \frac{3v\omega^2}{k^2 - \omega^2}(1 - \rho)^2 + \dots, \quad (6.1b)$$

$$A_1 = s - \frac{s}{2}(k^2 - \omega^2)(1 - \rho)^2 + v(1 - \rho)^3 + \dots. \quad (6.1c)$$

Now AdS/CFT tells us that the leading mode of A_1 should be identified with the source from the QFT perspective and with this we conclude that sourceless excitations have $s = 0$. We can easily impose this by defining

$$A_\rho = (1 - \rho)\hat{A}_\rho, \quad (6.2a)$$

$$\alpha_\rho = (1 - \rho)\hat{\alpha}_\rho, \quad (6.2b)$$

$$A_1 = (1 - \rho)^2\hat{A}_1, \quad (6.2c)$$

and demanding Dirichlet boundary conditions for the rescaled fields $\{\hat{A}_\rho, \hat{\alpha}_\rho, \hat{A}_1\}$. With all this, we thus define the function space for the GF framework as the space of regular functions $\{\hat{A}_\rho, \hat{\alpha}_\rho, \hat{A}_1\}$ satisfying Dirichlet boundary conditions at $\rho = 1$. This rescaling is consistent with demanding that any element in the function space has finite GF energy norm. Note that we choose to work directly in terms of the hatted variables, which in turn modifies the eigenvalue problem (3.17) and the energy norm (3.20) in a trivial manner. We also choose to perform a rescaling of the original eigenvalue problem in order to maintain a standard eigenvalue problem for the hatted variables. Note that as discussed in section 3.1, the CLM pseudospectrum is convergent as all outgoing modes with real frequency ω have infinite energy norm.

6.1.2 Setup in the MS framework

We study the pseudospectra of the eigenvalue problem (5.16) with respect to the inner product (5.15) and to have a well-defined problem we need to specify boundary conditions for the MS field ψ . Near the AdS boundary we have the following asymptotic behavior

$$\psi = s - \frac{3v}{k^2 - \omega^2}(1 - \rho) + \dots, \quad (6.3a)$$

$$\phi = iks - \frac{3ikv}{k^2 - \omega^2}(1 - \rho) + \dots, \quad (6.3b)$$

where s is the leading mode of A_1 in equation (6.1). Thus, for consistency we with the GF framework, we designate the function space as the space of regular functions $\{\psi, \phi\}$ satisfying Dirichlet boundary conditions at $\rho = 1$. This is consistent with demanding that any element in the function space has finite MS energy norm.

6.1.3 Numerical results

Now we turn onto the discussion of our numerical results. A detailed discussion of the numerical procedure can be found in appendix B. In this section we use a grid of 50 points and work with $5 \times \text{MachinePrecision}$ in both frameworks.

In figures 2-4 we present the CLMs pseudospectrum at frequencies $\omega = \{10^{-4}, 1, 10\}$ and the percentage of relative difference between the two approaches. We observe that both frameworks provide equivalent results, with a maximal relative difference (in the plotted region of the complex k plane) of $3 \cdot 10^{-7}\%$ for $\omega = 10^{-4}$, of $10^{-4}\%$ for $\omega = 1$ and of $5 \cdot 10^{-2}\%$ for $\omega = 10$. We associate this small difference to numerical error and do not assign physical significance to it.

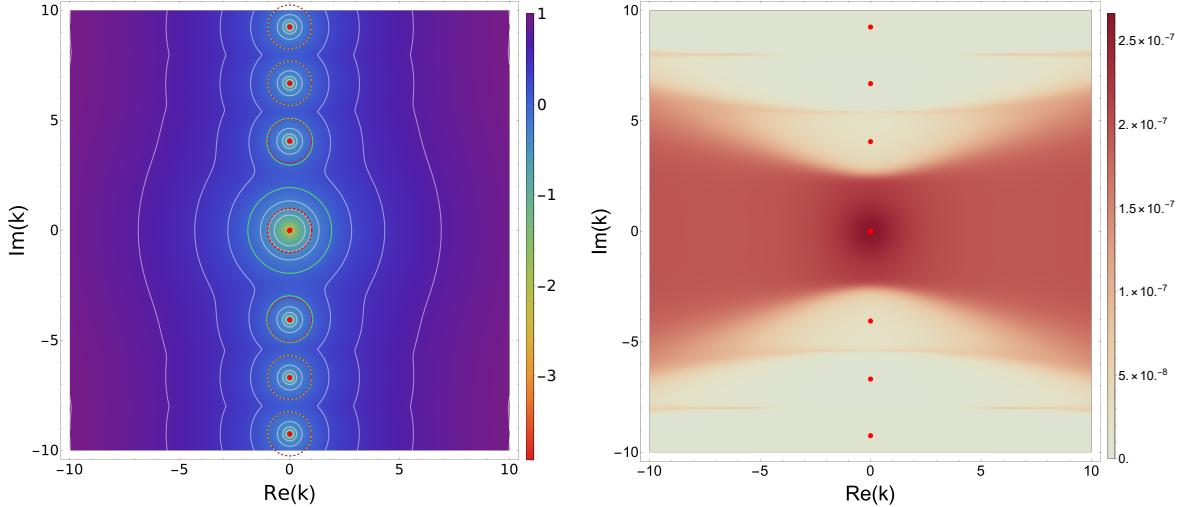


Figure 2: (Left) CLM pseudospectrum at $\omega = 10^{-4}$ for the $SAdS_{5+1}$ black brane. The white lines denote the boundaries of different ε -pseudospectra and the heat map corresponds to the logarithm in base 10 of the inverse of the norm of the resolvent. The green circles correspond to the boundaries of the $\varepsilon = 1$ -pseudospectra and the dashed red circles are circles of radius 1 centered on the CLMs. For the higher CLMs these coincide denoting spectral stability. (Right) Heatmap of the percentage difference between MS and GF frameworks. The red dots correspond to the CLMs.

Furthermore, the increase in the relative difference at higher frequencies can be understood as consequence of the increased spectral instability which amplifies numerical errors.

In figure 2 we observe that the non-hydro CLMs are increasingly stable at small frequencies, with the boundaries of the ε -pseudospectra around them resembling a set of concentric circles of radius ε . This matches our intuition as in the limit $\omega = 0$ all the CLMs, except the hydrodynamical one, are dual to glueball spectrum of a Hermitian unitary theory arising from the dimensional compactification on the

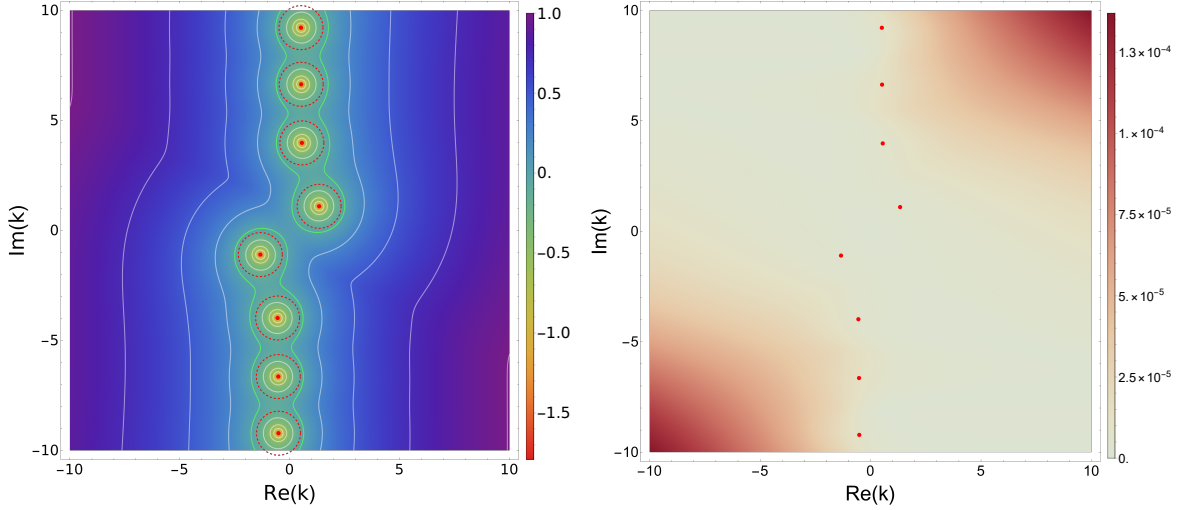


Figure 3: (Left) CLM pseudospectrum at $\omega = 1$ for the $SAdS_{5+1}$ black brane. The white lines denote the boundaries of different ε -pseudospectra and the heat map corresponds to the logarithm in base 10 of the inverse of the norm of the resolvent. The green circles correspond to the boundaries of the $\varepsilon = 1$ -pseudospectra and the dashed red circles are circles of radius 1 centered on the CLMs. Notably, the CLMs showcase mild spectral instability. (Right) Heatmap of the percentage difference between MS and GF frameworks. The red dots correspond to the CLMs.

thermal circle [67–69]; which should have a stable spectrum. The hydrodynamic mode becomes a pole skipping mode at $\omega = 0$ and thus leaves the physical spectrum, hence it need not be stable as ω is reduced. To quantify the spectral instability, we plot the condition numbers as a function of ω in the left panel of figure 5 for the hydro CLM and the first two non-hydro CLMs.⁹ Remarkably we observe that while non-hydro CLMs have monotonically increasing condition numbers, the condition number of the hydro CLM is non-monotonic, it decreases to a minimum value before increasing. This indicates that, while for the non-hydro CLMs the instability always increases with ω , for the hydro CLM the situation is more subtle: there is first a sharp decrease in instability up to some minimum value and only after that do we observe that the instability increases with ω .

The increasing instability of the hydrodynamic CLMs at small ω suggests that in the CLM picture, the hydrodynamic description is strongly dependent on small perturbations at small frequency. Indeed this is what one would expect as a consequence of the pole collision taking place between the CLMs at $\omega = 0$. The existence of a pole collision at $\omega = 0$ can be seen from the fact that the hydro CLMs follow a

⁹The computation of the condition numbers in the GF approach is numerically too intensive and thus we have chosen to calculate the condition numbers in the MS approach for simplicity. The equivalence between both approaches guarantees that results are equivalent.

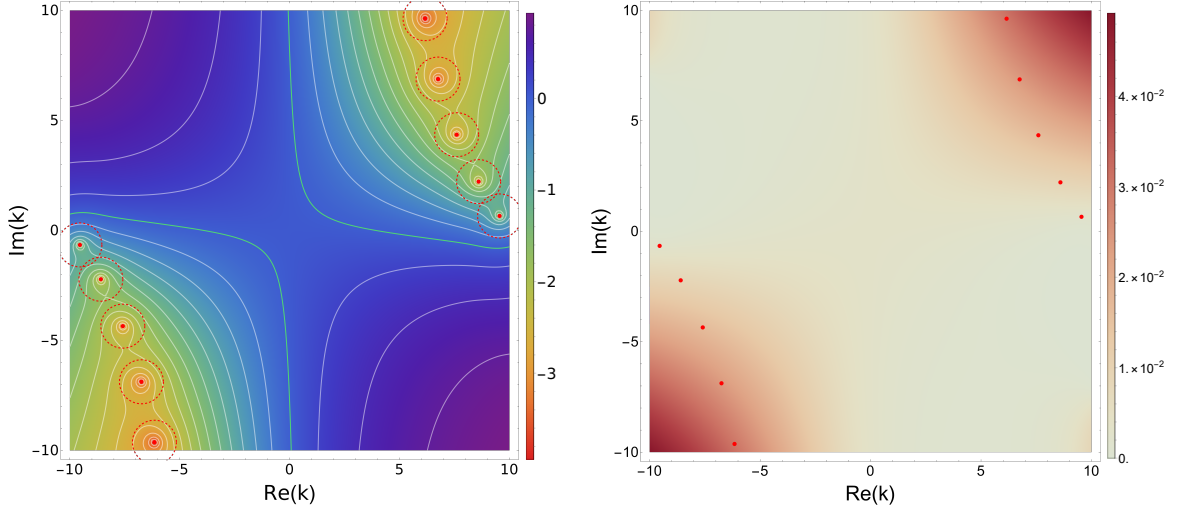


Figure 4: (Left) CLM pseudospectrum at $\omega = 10$ for the $SAdS_{5+1}$ black brane. The white lines denote the boundaries of different ϵ -pseudospectra and the heat map corresponds to the logarithm in base 10 of the inverse of the norm of the resolvent. The green circles correspond to the boundaries of the $\epsilon = 1$ -pseudospectra and the dashed red circles are circles of radius 1 centered on the CLMs. Notably, the CLMs showcase spectral instability. (Right) Heatmap of the percentage difference between MS and GF frameworks. The red dots correspond to the CLMs.

Puiseux series around $\omega = 0$ of the form

$$k_{\pm}(\omega) = \pm\sqrt{i\omega/D} + O(\omega) \quad (6.4)$$

with D the diffusion constant. This implies that $\omega = 0$ is an exceptional point of second order where k_{\pm} coalesce and the eigenvalue problem becomes non-diagonalizable. Exceptional points are characterized by their increased spectral instability: for sufficiently small ϵ the boundary of ϵ -pseudospectrum is given by a circle of radius $\epsilon^{1/p}$ with p the order of the exceptional point [77]. Then, as the pseudospectrum changes continuously with ω , the increased spectral instability of the exceptional point must leave a non-trivial imprint at small finite ω . This can be seen explicitly by writing the hydrodynamic condition number $\kappa_0(\omega)$ as the supremum over perturbations V

$$\kappa_0(\omega) = \lim_{\epsilon \rightarrow 0} \sup_{\|V\| < \epsilon} \left| \frac{k_{\pm}(\omega; \epsilon) - k_{\pm}(\omega)}{\epsilon} \right|, \quad (6.5)$$

with $k_{\pm}(\omega; \epsilon)$ the perturbed CLMs.¹⁰ Then it follows that if we construct a perturbation V whose effect is to shift $\omega \rightarrow \epsilon$, the hydrodynamic condition number must

¹⁰Note that due to the symmetries of the pseudospectrum the condition number of k_+ coincides with that of k_- , hence we use κ_0 to denote both

satisfy the following bound

$$\kappa_0(\omega) \geq \lim_{\epsilon \rightarrow 0} \left| \frac{k_{\pm}(\omega + \epsilon) - k_{\pm}(\omega)}{\epsilon} \right| \approx \lim_{\epsilon \rightarrow 0} \left| \frac{\sqrt{i(\omega + \epsilon)/D} - \sqrt{i\omega/D}}{\epsilon} \right| \approx \frac{1}{\sqrt{2D\omega}}. \quad (6.6)$$

Hence, the existence of the exceptional point of order 2 implies that at small ω , $\kappa_0(\omega)$ must diverge at least as fast as $1/\sqrt{\omega}$. In the right panel of figure 5, we explicitly check this by plotting $\log_{10}(\kappa_0)$ against $\log_{10}(\omega)$. We find that the condition number diverges as $\kappa_0 \propto \omega^{-1/2}$.

We claim that the instability of the hydro CLMs at small ω is simply signaling the non-analytic behavior in ω resulting from a pole collision. This suggests that pseudospectra could predict the existence of pole collisions as in their vicinity there is enhanced spectral instability. We stress that the instability of the hydro CLMs is in agreement with the expectation from hydrodynamics. The presence of the non-analytic behavior in the CLM description of diffusion alone is what makes the system very susceptible to small perturbations. From a physical standpoint, the increased instability is indicating the presence of an exceptional point and signaling that perturbations are enhanced in its vicinity. Thus, the instability is purely of hydrodynamic origin and is not directly related to the realization of this diffusive mode in the black hole background.

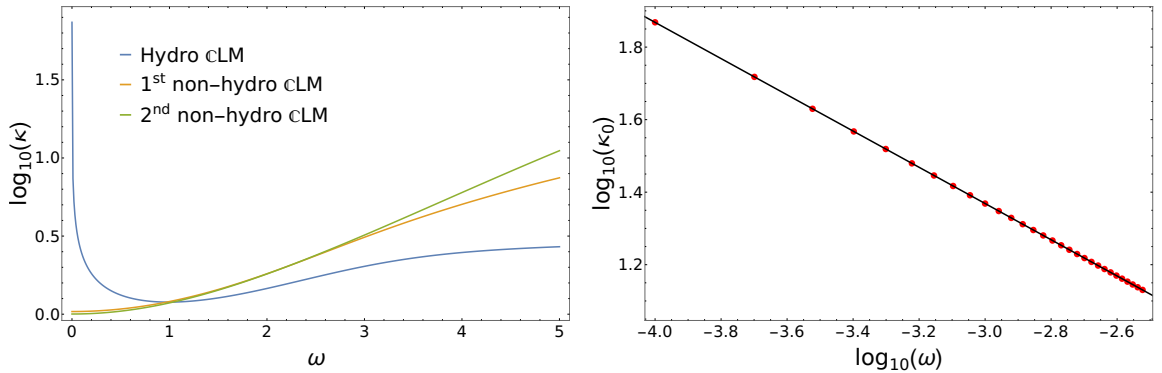


Figure 5: (Left) Condition numbers for the hydro CLM and the first two non-hydro CLMs as a function of the frequency ω for the SAdS₅₊₁ black brane. (Right) Plot of the hydrodynamic CLM condition number at small frequency ω for the SAdS₅₊₁ black brane. The red dots denote the numerical values of the condition numbers and the black line is the fit $\log_{10}(\kappa_0) = -0.130 - 0.500 \log_{10}(\omega)$.

6.2 QNFs of SAdS₅₊₁ black brane

Now we turn to the study of the spectral stability of the QNFs of the longitudinal sector of a gauge field with action (1.1) in the (5+1)-dimensional black brane in-

troduced in the previous subsection, whose metric is given by equation (1.2) with $d = 5$.

6.2.1 Boundary conditions in the GF framework

In the GF framework we study the pseudospectra of the eigenvalue problem (3.5) subject to the constraint (3.6) with respect to the inner product (3.10). As before, to define the boundary conditions we follow AdS/CFT as our guideline. We impose regularity on the event horizon to select infalling modes and on the AdS boundary we demand that there is no source from the point of view of the dual QFT. Solving the equations of motion in the $\rho \rightarrow 1$ region for modes with momentum k and frequency ω we find the following asymptotic behavior of the fields depending only on two parameters $\{s, v\}$

$$A_\rho = -i\omega s(1 - \rho) + \frac{3i\omega v}{k^2 - \omega^2}(1 - \rho)^2 + \dots, \quad (6.7a)$$

$$\alpha_\rho = -k^2 s(1 - \rho) + \frac{3k^2 v}{k^2 - \omega^2}(1 - \rho)^2 + \dots, \quad (6.7b)$$

$$A_t = s - \frac{s}{2}(k^2 - \omega^2)(1 - \rho)^2 + v(1 - \rho)^3 + \dots. \quad (6.7c)$$

AdS/CFT identifies the leading mode of A_t with the source and thus sourceless excitations have $s = 0$. This can be imposed by defining

$$A_\rho = (1 - \rho)\hat{A}_\rho, \quad (6.8a)$$

$$\alpha_\rho = (1 - \rho)\hat{\alpha}_\rho, \quad (6.8b)$$

$$A_t = (1 - \rho)^2 \hat{A}_t, \quad (6.8c)$$

and demanding Dirichlet boundary conditions for the rescaled fields $\{\hat{A}_\rho, \hat{\alpha}_\rho, \hat{A}_t\}$. We thus define the function space as the space of regular functions $\{\hat{A}_\rho, \hat{\alpha}_\rho, \hat{A}_t\}$ satisfying Dirichlet boundary conditions at $\rho = 1$. This rescaling is consistent with demanding that any element in the function space has finite GF energy norm. As for the CLMs, we choose to work directly in terms of the hatted variables and we rescale the original eigenvalue problem to maintain a standard eigenvalue problem for the hatted variables.

6.2.2 Boundary conditions in the MS framework

Now, we study the pseudospectra of the eigenvalue problem (4.6) with respect to the inner product (4.12). Near the AdS boundary we have the following asymptotic behavior for the fields

$$\psi = s - \frac{3v}{k^2 - \omega^2}(1 - \rho) + \dots, \quad (6.9a)$$

$$\phi = -i\omega s + \frac{3i\omega v}{k^2 - \omega^2}(1 - \rho) + \dots, \quad (6.9b)$$

where s is the leading mode of A_t in equation (6.7). Thus, for consistency with the GF framework, we designate the function space as the space of regular functions $\{\psi, \phi\}$ satisfying Dirichlet boundary conditions at $\rho = 1$. This is consistent with demanding that any element in the function space has finite MS energy norm.

6.2.3 Numerical results

Now we present our numerical results for the QNF pseudospectra in the GF and MS approaches. We use a grid of 50 points and work with $5 \times \text{MachinePrecision}$ in both frameworks.

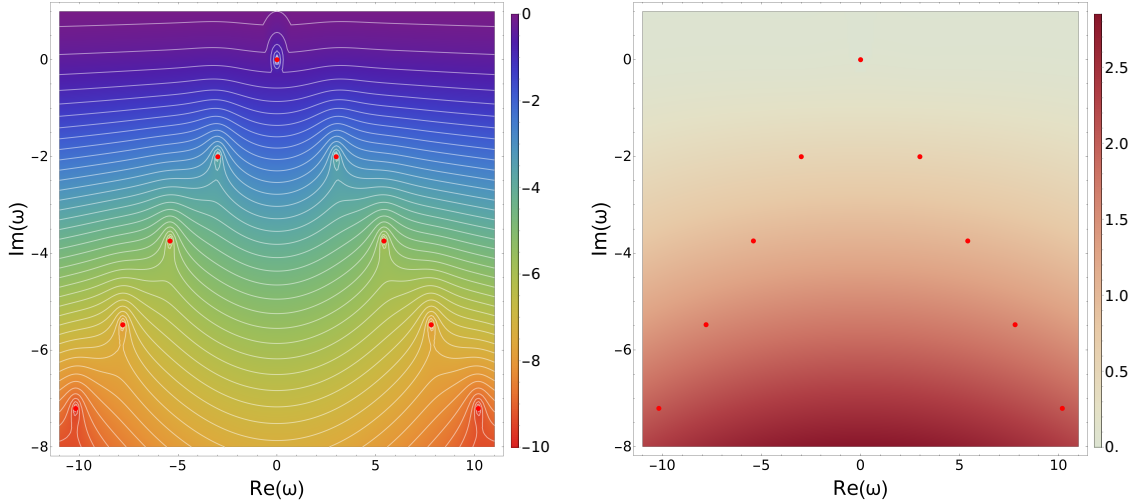


Figure 6: (Left) QNF pseudospectrum at $k = 10^{-4}$ for the SAdS_{5+1} black brane. The white lines denote the boundaries of different ε -pseudospectra and the heat map corresponds to the logarithm in base 10 of the inverse of the norm of the resolvent. (Right) Heatmap of the percentage difference between MS and GF frameworks. The red dots correspond to the QNFs.

In figures 6-8 we present the QNF pseudospectrum at $k = 10^{-4}$, $k = 1$ and $k = 10$ and the percentage of relative difference between the MS and GF approaches. We observe that both frameworks provide equivalent results, with a maximal relative difference (in the plotted region of the complex ω plane) of approximately 3% in all cases. As for the CLMs, this relative difference is associated with the numerical procedure. However, in this case it is significantly larger as the QNFs are much more unstable. Notably, we also find that the relative difference increases towards the lower half of the complex ω plane where the QNFs are seen to be more spectrally unstable, further confirming that the observed discrepancy is indeed a numerical artifact.

We observe that QNFs are more spectrally stable as they get closer to the real axis. Moreover the spectral instability of the QNFs far away from the real axis is much greater than the spectral instability observed for CLMs. This has extensively

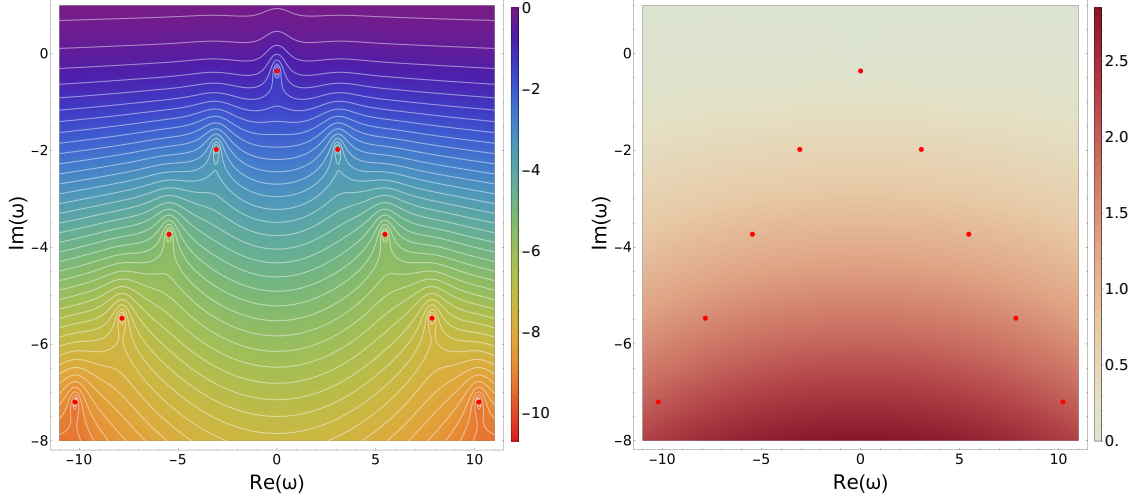


Figure 7: (Left) QNF pseudospectrum at $k = 1$ for the $SAdS_{5+1}$ black brane. The white lines denote the boundaries of different ε -pseudospectra and the heat map corresponds to the logarithm in base 10 of the inverse of the norm of the resolvent. (Right) Heatmap of the percentage difference between MS and GF frameworks. The red dots correspond to the QNFs.

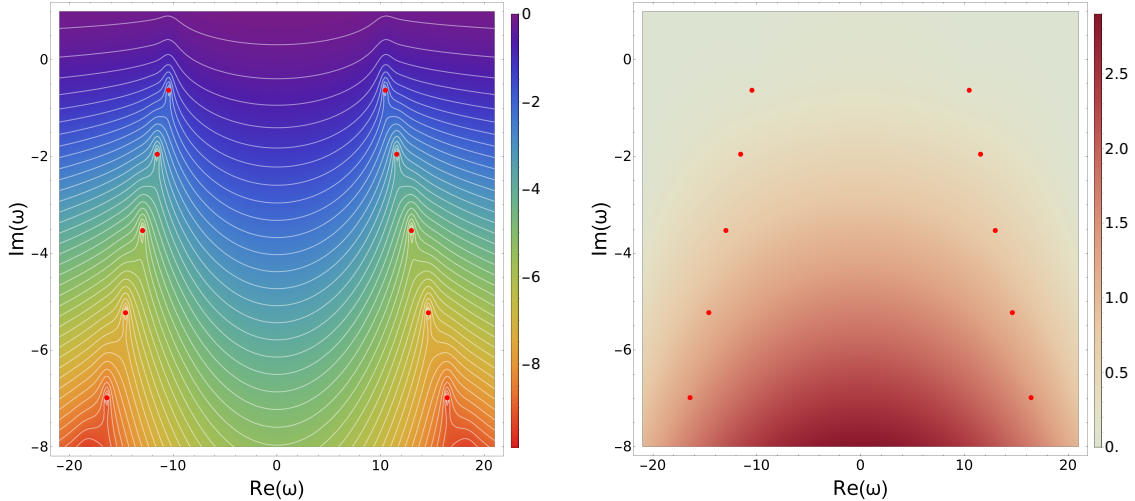


Figure 8: (Left) QNF pseudospectrum at $k = 10$ for the $SAdS_{5+1}$ black brane. The white lines denote the boundaries of different ε -pseudospectra and the heat map corresponds to the logarithm in base 10 of the inverse of the norm of the resolvent. (Right) Heatmap of the percentage difference between MS and GF frameworks. The red dots correspond to the QNFs.

been observed in other setups and seems to be closely related to the lack of convergence of the QNF pseudospectrum [17, 76]. In detail, as we go deeper in the complex ω plane, outgoing modes are increasingly close in the continuum function space to a

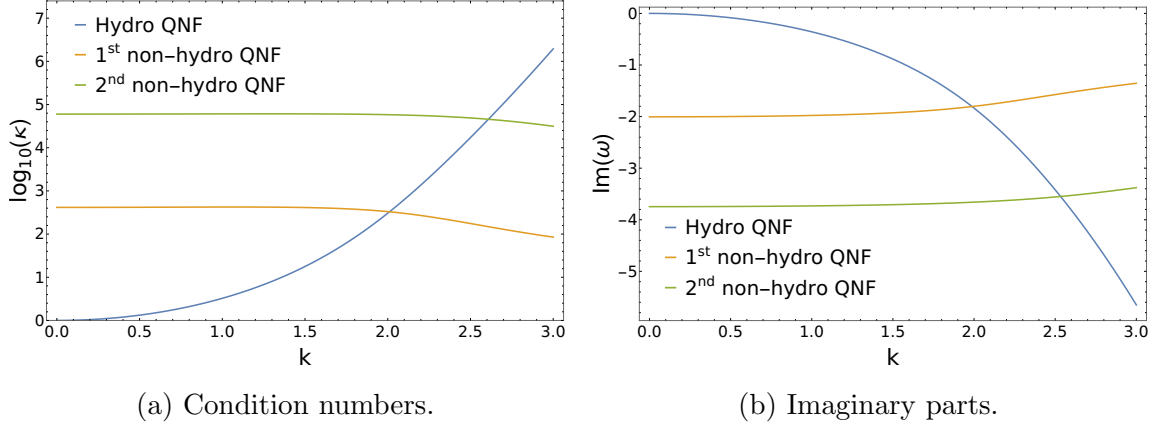


Figure 9: Condition numbers and imaginary part of the hydro QNF and the first two non-hydro QNFs as a function of the momentum k for the SAdS_{5+1} black brane. We see that the hydro QNF becomes more unstable than the non-hydro QNFs at values of the momentum similar to those for which the imaginary part of the former crosses that of the latter.

sum of Chebyshev polynomials living in our truncated space.¹¹ Hence those modes behave as ε -pseudoeigenmodes with $\varepsilon = \varepsilon(N)$. Thus the pseudospectrum does not converge on the entire complex plane, only above the band $\text{Im}(\omega) > -\pi T = -5/4$, and it showcases large instabilities deep in the lower half plane. We want to stress however, that this lack of convergence is a fundamental feature of the problem and consequently not unphysical. In the continuum limit we cannot eliminate outgoing modes with an energy norm derived from a theory of two derivatives, such as GR. Indeed, as argued in [76] to properly define the set of all QNMs one needs a Sobolev norm with an infinite number of derivatives. Hence we can interpret the lack of convergence as a hint of the breakdown of GR as a two-derivative EFT signaling the need for higher derivative corrections. Within this picture, we then view the grid size N as an UV cutoff telling us the smallest scale one can possibly discern within the two-derivative EFT. Thus we claim that the results are physical but computed at a given value of the UV cutoff. Also, it is worth mentioning that for sufficiently small k the hydrodynamic mode is in the convergent region $\text{Im}(\omega) > -\pi T = -5/4$ and its stability properties do not depend on the cutoff. This is checked numerically in appendix D.

Regarding the hydrodynamic mode, we observe that it is stable in the limit of $k \rightarrow 0$. In fact, for $k = 10^{-4}$ we find that its condition number is $\kappa_{\text{hydro}} = 1 + 10^{-8}$. This implies that the hydrodynamic description is stable at sufficiently small momenta, indicating that models differing by small perturbations predict the same hydrodynamics up to errors of the same order. This matches the physical

¹¹Here by close we mean that the energy norm of the difference becomes smaller

expectations that the hydrodynamic description should be universal. On the other hand, non-hydro QNFs are always unstable. In figure 9 we plot the condition number as a function of k for the hydro QNF and the first two non-hydro QNFs. Remarkably, we observe that while the non-hydro QNFs become more stable with k (they get closer to the real axis) the hydro QNF becomes more unstable (it gets further away to the real axis). Furthermore, we can see that the value of k at which the hydro QNF becomes more unstable than the non-hydro QNFs, is close to the k for which the imaginary part of the former becomes larger in absolute value than that of the latter. Lastly, note that the rapid increase of $\kappa_{\text{hydro}}(k)$ implies that the hydrodynamic description rapidly becomes unstable as it feels shorter scales, confirming that the QNF instability starts playing a role only when start feeling the UV.

6.3 CLMs of SAdS_{4+1} black brane

In this subsection we study the CLMs of the longitudinal sector of a gauge field with action (1.1) in a $(4+1)$ -dimensional black brane with metric (1.2) with $d = 4$. Recall that we work in units where the temperature is fixed to $T = 1/\pi$.

6.3.1 Boundary conditions in the GF framework

In the GF framework we study the pseudospectra of the eigenvalue problem (3.17) subject to the constraint (3.18) with respect to the inner product (3.20). For the boundary conditions, we impose regularity on the event horizon to select infalling modes and on the AdS boundary we demand that there is no source from the point of view of the dual QFT. Solving the equations of motion in the $\rho \rightarrow 1$ region for modes with momentum k and frequency ω and we find the following asymptotic behavior of the fields depending only on two parameters $\{s, v\}$

$$A_\rho = \frac{iks}{2}(1 - \rho) + \frac{2ikv}{k^2 - \omega^2}(1 - \rho) + iks(1 - \rho) \log(1 - \rho) + \dots, \quad (6.10a)$$

$$\alpha_\rho = -\frac{s\omega^2}{2}(1 - \rho) - \frac{2v\omega^2}{k^2 - \omega^2}(1 - \rho) - s\omega^2(1 - \rho) \log(1 - \rho) + \dots, \quad (6.10b)$$

$$A_1 = s + v(1 - \rho)^2 + \frac{s}{2}(k^2 - \omega^2)(1 - \rho)^2 \log(1 - \rho) + \dots, \quad (6.10c)$$

where the AdS/CFT dictionary establishes that s is the source of the QFT perspective. With this we conclude that sourceless excitations have $s = 0$ and thus we impose this by defining

$$A_\rho = \hat{A}_\rho, \quad (6.11a)$$

$$\alpha_\rho = \hat{\alpha}_\rho, \quad (6.11b)$$

$$A_1 = (1 - \rho)\hat{A}_1, \quad (6.11c)$$

and demanding Dirichlet boundary conditions for the hatted fields $\{\hat{A}_\rho, \hat{\alpha}_\rho, \hat{A}_1\}$. Thus we define the function space for the as the space of regular functions $\{\hat{A}_\rho, \hat{\alpha}_\rho, \hat{A}_1\}$ satisfying Dirichlet boundary conditions at $\rho = 1$. This rescaling is consistent with demanding that any element in the function space has finite GF energy norm. As before, we work directly in terms of the hatted variables and rescale the original eigenvalue problem to have a standard eigenvalue problem for the hatted variables.

6.3.2 Setup in the MS framework

We study the pseudospectra of the eigenvalue problem (5.16) with respect to the inner product (5.15) and to have a well-defined problem we need to specify boundary conditions for the MS field ψ .

Near the AdS boundary we have the following asymptotic behavior

$$\psi = \frac{ks}{2} \sqrt{1-\rho} + \frac{2kv}{k^2 - \omega^2} \sqrt{1-\rho} + ks\sqrt{1-\rho} \log(1-\rho) + \dots, \quad (6.12a)$$

$$\phi = \frac{isk^2}{2} \sqrt{1-\rho} + \frac{2ivk^2}{k^2 - \omega^2} \sqrt{1-\rho} + isk^2\sqrt{1-\rho} \log(1-\rho) + \dots, \quad (6.12b)$$

where s is the leading mode of A_1 in equation (6.10). Thus, for consistency we with the GF framework we designate the function space as the space of regular functions $\{\hat{\psi}, \hat{\phi}\}$, where the hatted fields are defined by

$$\psi = \sqrt{1-\rho} \hat{\psi}, \quad (6.13a)$$

$$\phi = \sqrt{1-\rho} \hat{\phi}, \quad (6.13b)$$

so that the non-analytic factors of $\sqrt{1-\rho}$ present in $\{\psi, \phi\}$ disappear.

This is precisely the case in which the boundary term in the energy norm of the master scalar prevents positive definiteness. We base our analysis therefore on the norm (4.9) and inner product (4.12).

6.3.3 Numerical results

Now we turn onto the discussion of our numerical results. In this section we use a grid of 50 points and work with $5 \times \text{MachinePrecision}$ in both frameworks.

We note that for the master scalar, in this case the differential operator whose spectrum we are studying diverges as $(1-\rho)^{-1}$ towards the AdS boundary. This issue could be addressed by working with a generalized eigenvalue problem obtained from multiplying our standard one by $(1-\rho)$. However, to facilitate our analysis, we choose to maintain the standard eigenvalue problem and instead replace the rows of the discretized operator corresponding to the AdS boundary with an expression obtained by performing an asymptotic expansion around that boundary. Then, if we remove the terms that vanish when we fix our desired boundary conditions from the asymptotic expansion, we get a standard eigenvalue problem without any divergences. At any finite gridsize N , this procedure introduces numerical errors, which

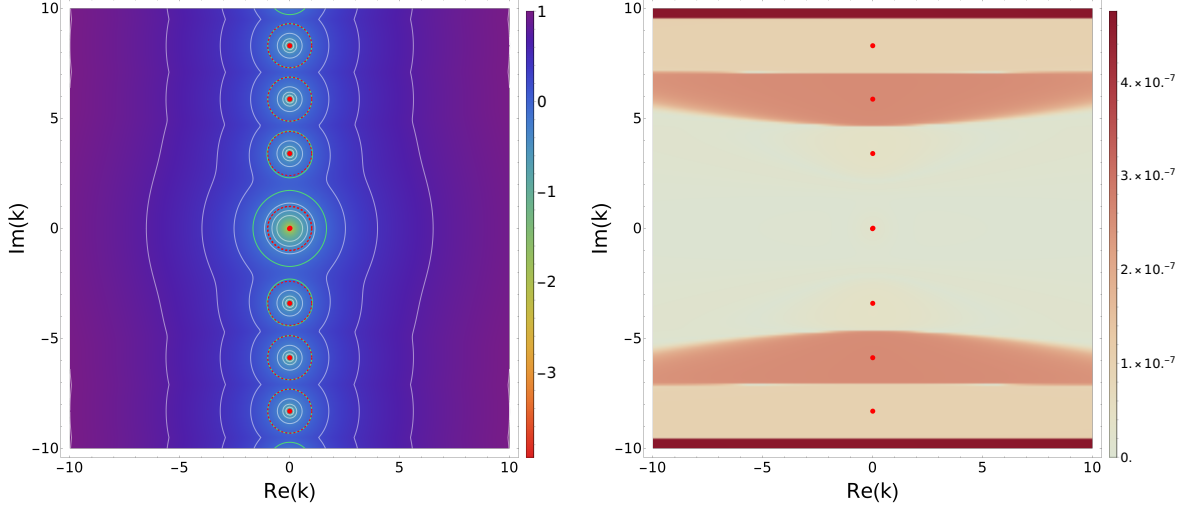


Figure 10: (Left) CLM pseudospectrum at $\omega = 10^{-4}$ for the $SAdS_{4+1}$ black brane. The white lines denote the boundaries of different ϵ -pseudospectra and the heat map corresponds to the logarithm in base 10 of the inverse of the norm of the resolvent. The green circles correspond to the boundaries of the 1-pseudospectra and the dashed red circles are circles of radius 1 centered on the CLMs. For the higher CLMs these coincide denoting spectral stability. (Right) Heatmap of the percentage difference between MS and GF frameworks. The red dots correspond to the CLMs.

enhance the relative difference between MS and GF approaches with respect to the results found for $SAdS_{5+1}$. Nonetheless as N increases the numerical error associated with changing the discretized operator becomes smaller and thus the relative difference between frameworks is also reduced (see appendix C for an explicit showcase of this phenomenon in the context of QNFs). This can be understood by noting that one can think that our procedure is altering the original operator in the region between the boundary and the second grid point. Hence when this region becomes smaller as N increases, the change in the original operator decreases.

In figures 10-12 we plot the pseudospectra and the relative difference between GF and MS frameworks for $\omega = \{10^{-4}, 1, 10\}$ and in figure 13 we plot the condition numbers for the hydro and the first non-hydro CLM. We observe great agreement between both approaches with relative differences of only 0.3% in the worst case. As mentioned above, this increase in the relative difference is associated with the procedure employed to remove the divergence in the MS framework. The overall results are qualitatively identical to those found for AdS_{5+1} in section 6.1.3. Hence for the sake of brevity we do not repeat the discussion here.

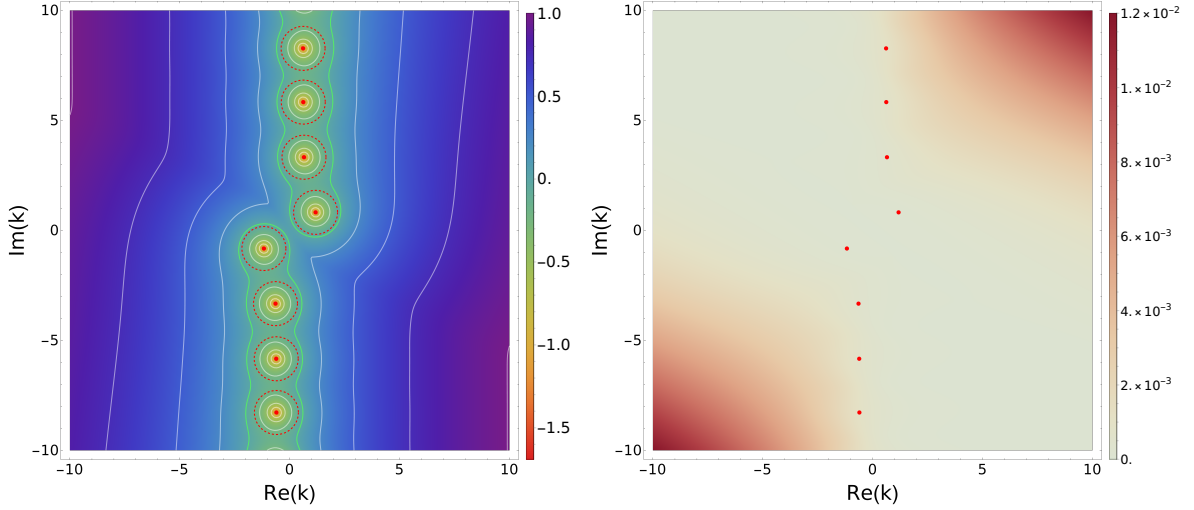


Figure 11: (Left) CLM pseudospectrum at $\omega = 1$ for the $SAdS_{4+1}$ black brane. The white lines denote the boundaries of different ϵ -pseudospectra and the heat map corresponds to the logarithm in base 10 of the inverse of the norm of the resolvent. The green circles correspond to the boundaries of the 1-pseudospectra and the dashed red circles are circles of radius 1 centered on the CLMs. Notably, the CLMs showcase mild spectral instability. (Right) Heatmap of the percentage difference between MS and GF frameworks. The red dots correspond to the CLMs.

6.4 QNFs of $SAdS_{4+1}$ black brane

Now we analyze the spectral stability of the QNFs of the longitudinal sector of a gauge field with action (1.1) in the (4+1)-dimensional black brane introduced in the previous subsection, whose metric is given by equation (1.2) with $d = 4$.

We note that this setup has already been considered in Eddington-Finkelstein coordinates in [26]. In particular, in their notation our results correspond to the $Q = 0$ results for the diffusive sector. We believe our presentation offers new insights into the problem. In particular, the stability analysis becomes more transparent as we have a standard eigenvalue problem rather than a generalized one. This allows us to properly quantify the stability of the hydro mode.

6.4.1 Boundary conditions in the GF framework

In the GF framework we study the pseudospectra of the eigenvalue problem (3.5) subject to the constraint (3.6) with respect to the inner product (3.10). We impose regularity on the event horizon to select infalling modes and on the AdS boundary we demand that there is no source. Solving the equations of motion in the $\rho \rightarrow 1$ region for modes with momentum k and frequency ω we find the following asymptotic

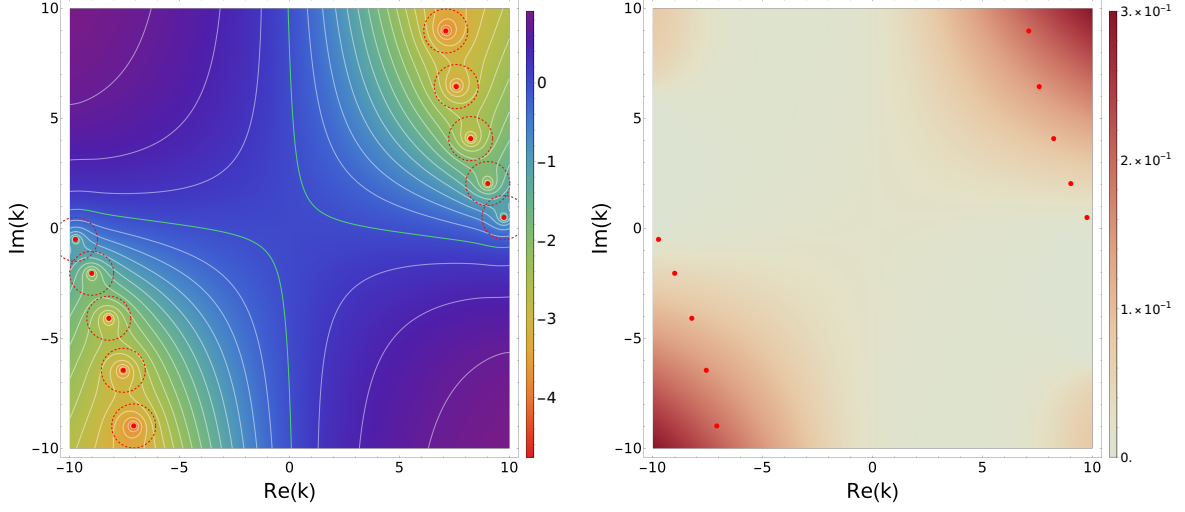


Figure 12: (Left) CLM pseudospectrum at $\omega = 10$ for the SAdS₄₊₁ black brane. The white lines denote the boundaries of different ε -pseudospectra and the heat map corresponds to the logarithm in base 10 of the inverse of the norm of the resolvent. The green circles correspond to the boundaries of the 1-pseudospectra and the dashed red circles are circles of radius 1 centered on the CLMs. Notably, the CLMs showcase spectral instability. (Right) Heatmap of the percentage difference between MS and GF frameworks. The red dots correspond to the CLMs.

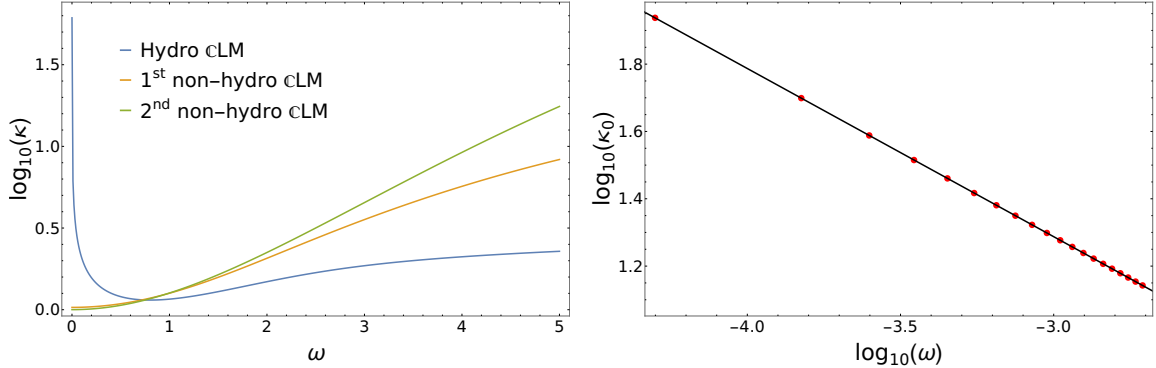


Figure 13: (Left) Condition numbers for the hydro CLM and the first two non-hydro CLMs as a function of the frequency ω for the SAdS₄₊₁ black brane. (Right) Plot of the hydrodynamic CLM condition number at small frequency ω for the SAdS₄₊₁ black brane. The red dots denote the numerical values of the condition numbers and the black line is the fit $\log_{10}(\kappa_0) = -0.211 - 0.500 \log_{10}(\omega)$.

behavior of the fields

$$A_\rho = \frac{i\omega s}{2}(1 - \rho) + \frac{2i\omega v}{k^2 - \omega^2}(1 - \rho) + i\omega s(1 - \rho) \log(1 - \rho) + \dots, \quad (6.14a)$$

$$\alpha_\rho = \frac{sk^2}{2}(1 - \rho) + \frac{2vk^2}{k^2 - \omega^2}(1 - \rho) + sk^2(1 - \rho) \log(1 - \rho) + \dots, \quad (6.14b)$$

$$A_t = s + v(1 - \rho)^2 + \frac{s}{2}(k^2 - \omega^2)(1 - \rho)^2 \log(1 - \rho) \dots, \quad (6.14c)$$

where s is the source which we should set to zero. We can impose this by defining

$$A_\rho = \hat{A}_\rho, \quad (6.15a)$$

$$\alpha_\rho = \hat{\alpha}_\rho, \quad (6.15b)$$

$$A_t = (1 - \rho)\hat{A}_t, \quad (6.15c)$$

and demanding Dirichlet boundary conditions for the rescaled fields $\{\hat{A}_\rho, \hat{\alpha}_\rho, \hat{A}_t\}$. We thus define the function space as the space of regular functions $\{\hat{A}_\rho, \hat{\alpha}_\rho, \hat{A}_t\}$ satisfying Dirichlet boundary conditions at $\rho = 1$. This rescaling is consistent with demanding that any element in the function space has finite GF energy norm. We work directly in terms of the hatted variables and we rescale the original eigenvalue problem to maintain a standard eigenvalue problem for the hatted variables.

6.4.2 Boundary conditions in the MS framework

We study the pseudospectra of the eigenvalue problem (4.6) with respect to the inner product (4.12). Near the AdS boundary we have the following asymptotic behavior for the fields

$$\psi = \frac{\omega s}{2} \sqrt{1 - \rho} + \frac{2\omega v}{k^2 - \omega^2} \sqrt{1 - \rho} + \omega s \sqrt{1 - \rho} \log(1 - \rho) + \dots, \quad (6.16a)$$

$$\phi = -\frac{is\omega^2}{2} \sqrt{1 - \rho} - \frac{2iv\omega^2}{k^2 - \omega^2} \sqrt{1 - \rho} - is\omega^2 \sqrt{1 - \rho} \log(1 - \rho) + \dots, \quad (6.16b)$$

where s is the leading mode of A_t in equation (6.14). Hence, we designate the function space as the space of regular functions $\{\hat{\phi}, \hat{\psi}\}$, where the hatted fields are defined with the non-analytic $\sqrt{1 - \rho}$ factors removed

$$\psi = \sqrt{1 - \rho} \hat{\psi}, \quad (6.17a)$$

$$\phi = \sqrt{1 - \rho} \hat{\phi}. \quad (6.17b)$$

6.4.3 Numerical results

Now we turn onto the discussion of our numerical results. In this section we use a grid of 150 points and work with $7 \times \text{MachinePrecision}$ in both frameworks. We note that as for the CLMs in SAdS_{4+1} , we have a divergent operator in the MS framework and we deal with that divergence as explained previously in section 6.3.3.

In figures 14–16 we plot the pseudospectra and the relative difference between GF and MS frameworks for $k = \{10^{-4}, 1, 10\}$ and in figure 17 we plot the condition numbers for the hydro and the first non-hydro QNF. We note that as for the CLMs we have that our procedure of dealing with the divergence in the MS approach introduces numerical errors, which enhance the relative difference between MS and GF approaches. As before, the relative difference decreases as the grid becomes denser as we explicitly shown in appendix C. Regarding the final results, we find qualitatively the same picture as for AdS_{5+1} in section 6.2.3, hence for the sake of brevity we do not repeat the discussion here.

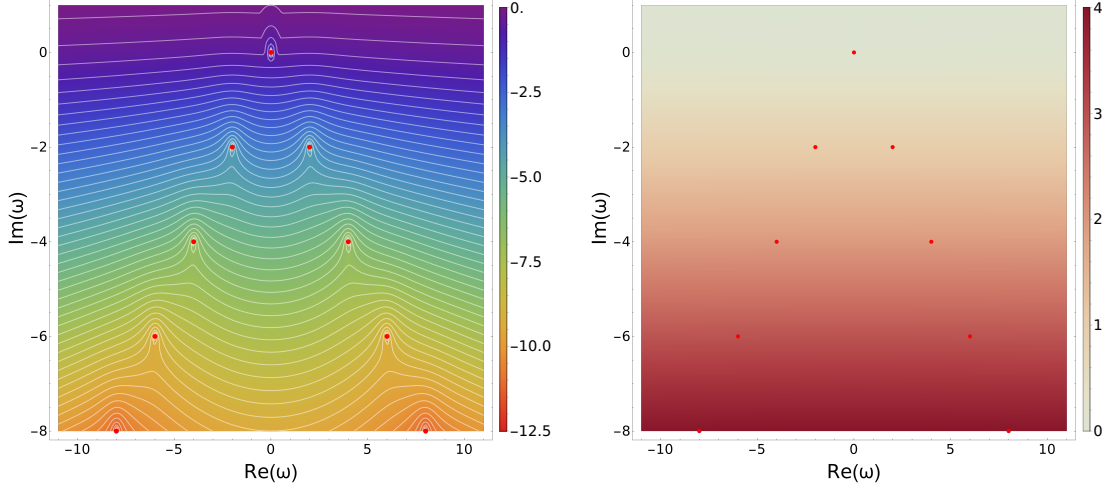


Figure 14: (Left) QNF pseudospectrum at $k = 10^{-4}$ for the $SAdS_{4+1}$ black brane. The white lines denote the boundaries of different ε -pseudospectra and the heat map corresponds to the logarithm in base 10 of the inverse of the norm of the resolvent. (Right) Heatmap of the percentage difference between MS and GF frameworks. The red dots correspond to the QNFS.

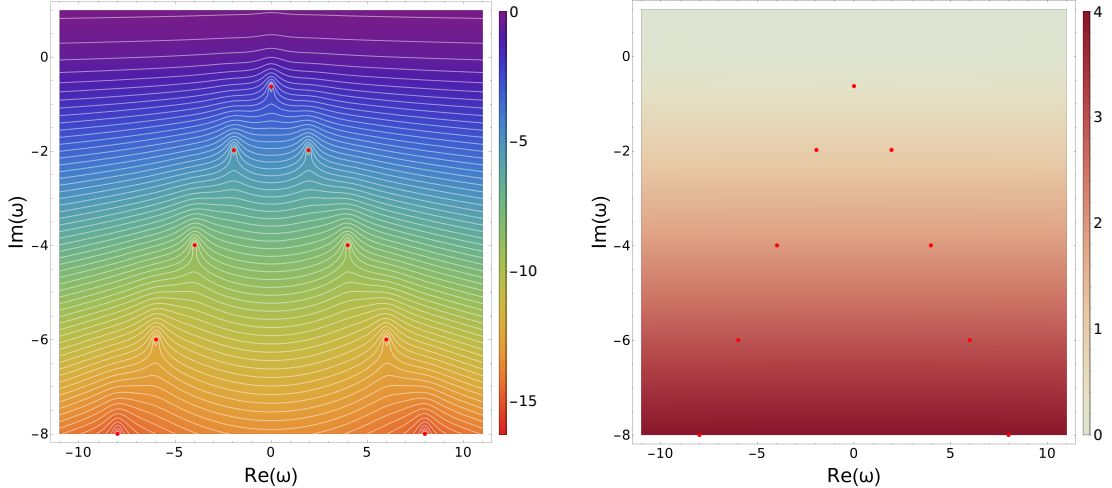


Figure 15: (Left) QNF pseudospectrum at $k = 1$ for the $SAdS_{4+1}$ black brane. The white lines denote the boundaries of different ε -pseudospectra and the heat map corresponds to the logarithm in base 10 of the inverse of the norm of the resolvent. (Right) Heatmap of the percentage difference between MS and GF frameworks. The red dots correspond to the QNFS.

6.5 QNFs of $SAdS_{4+1}$ black hole

Finally we conclude by showcasing how our procedure can be applied to a spherical black hole. For concreteness we focus on the gauge field QNFs of spherical black hole

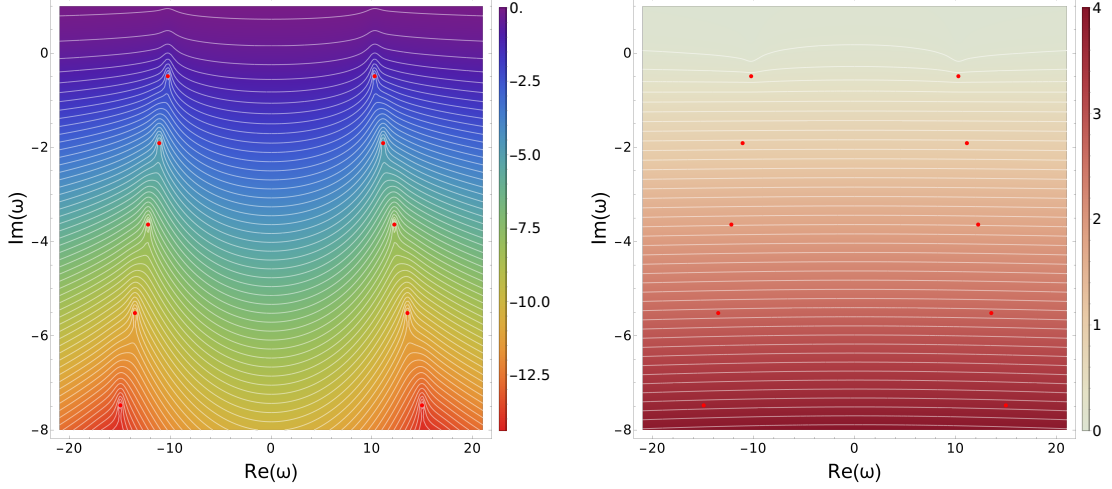


Figure 16: (Left) QNF pseudospectrum at $k = 10$ for the $SAdS_{4+1}$ black brane. The white lines denote the boundaries of different ε -pseudospectra and the heat map corresponds to the logarithm in base 10 of the inverse of the norm of the resolvent. (Right) Heatmap of the percentage difference between MS and GF frameworks. The red dots correspond to the QNFs.

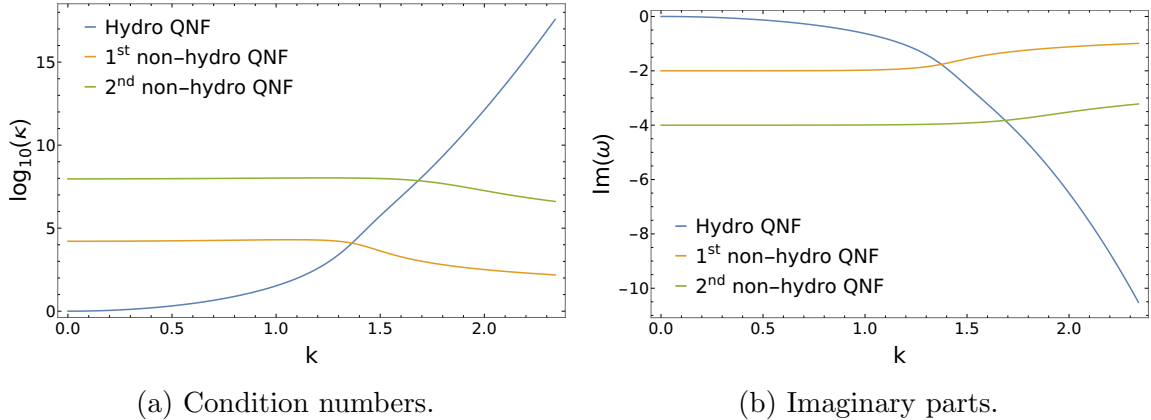


Figure 17: Condition numbers and imaginary part of the hydro QNF and the first two non-hydro QNFs as a function of the momentum k for the $SAdS_{4+1}$ black brane. We see that the hydro QNF becomes more unstable than the non-hydro QNFs at values of the momentum similar to those for which the imaginary part of the former crosses that of the latter.

in AdS_{4+1} . The corresponding metric in regular coordinates is given by:

$$ds^2 = \frac{1}{(1-\rho)^2}(-fdt^2 + 2r_h\beta dtd\rho + \frac{1-\beta^2}{f}r_h^2d\rho^2 + r_h^2d\Omega_2),$$

$$f = \frac{r_h^2}{l^2} + (1-\rho)^2 - \left(1 + \frac{r_h^2}{l^2}\right)(1-\rho)^4, \quad \beta = \left[1 + \frac{f}{(1-\rho)^5}\right]^{-1/2}, \quad (6.18)$$

where l is the AdS length scale and r_h is a constant with units of length. The Hawking temperature of these black holes is $T = (2\pi r_h)^{-1} + (r_h)/(\pi l^2)$. Unlike for the branes of the previous subsections, here r_h and l both enter non-trivially into the equations of motion and thus they cannot be simultaneously fixed without losing information. Hence we have a family of black holes labeled by the dimensionless ratio r_h/l . From the QFT point of view we see this as a consequence of the conformal symmetry of the UV. Now the dual QFT lives on a sphere and thus one can construct a dimensionless quantity to label state by combining the temperature and the radius of the sphere. Hence we have a continuous family of states labeled by a single parameter.

For the sake of brevity, here we focus on the $l = r_h = 1$ case and postpone discussing the behavior of the QNFs and pseudospectra as a function of the ratio r_h/l to future work.

6.5.1 Boundary conditions in the GF framework

In the GF framework we study the pseudospectra of the eigenvalue problem (3.5) subject to the constraint (3.6) with respect to the inner product (3.10). We define the boundary conditions following AdS/CFT as our guideline. We impose regularity on the event horizon to select infalling modes and on the AdS boundary we demand that there is no source. Solving the equations of motion in the $\rho \rightarrow 1$ region for modes with total angular momentum $\lambda^2 = L(2 + L)$ and frequency ω we find the following asymptotic behavior of the fields

$$A_\rho = \frac{i\omega s}{2}(1 - \rho) + \frac{2i\omega v}{\lambda^2 - \omega^2}(1 - \rho) + i\omega s(1 - \rho) \log(1 - \rho) + \dots, \quad (6.19a)$$

$$\alpha_\rho = \frac{s\lambda^2}{2}(1 - \rho) + \frac{2v\lambda^2}{\lambda^2 - \omega^2}(1 - \rho) + s\lambda^2(1 - \rho) \log(1 - \rho) + \dots, \quad (6.19b)$$

$$A_t = s + v(1 - \rho)^2 + \frac{s}{2}(\lambda^2 - \omega^2)(1 - \rho)^2 \log(1 - \rho) + \dots, \quad (6.19c)$$

where s is the source which we should set to zero. We can impose this by defining

$$A_\rho = \hat{A}_\rho, \quad (6.20a)$$

$$\alpha_\rho = \hat{\alpha}_\rho, \quad (6.20b)$$

$$A_t = (1 - \rho)\hat{A}_t, \quad (6.20c)$$

and demanding Dirichlet boundary conditions for the rescaled fields $\{\hat{A}_\rho, \hat{\alpha}_\rho, \hat{A}_t\}$. We thus define the function space as the space of regular functions $\{\hat{A}_\rho, \hat{\alpha}_\rho, \hat{A}_t\}$ satisfying Dirichlet boundary conditions at $\rho = 1$. This rescaling is consistent with demanding that any element in the function space has finite GF energy norm. We work directly in terms of the hatted variables and we rescale the original eigenvalue problem to maintain a standard eigenvalue problem for the hatted variables.

6.5.2 Boundary conditions in the MS framework

We study the pseudospectra of the eigenvalue problem (4.6) with respect to the inner product (4.12). Near the AdS boundary we have the following asymptotic behavior for the fields

$$\psi = \frac{\omega s}{2} \sqrt{1-\rho} + \frac{2\omega v}{\lambda^2 - \omega^2} \sqrt{1-\rho} + \omega s \sqrt{1-\rho} \log(1-\rho) + \dots, \quad (6.21a)$$

$$\phi = -\frac{is\omega^2}{2} \sqrt{1-\rho} - \frac{2iv\omega^2}{\lambda^2 - \omega^2} \sqrt{1-\rho} - is\omega^2 \sqrt{1-\rho} \log(1-\rho) + \dots, \quad (6.21b)$$

where s is the leading mode of A_t in equation (6.19). Hence, we designate the function space as the space of regular functions $\{\hat{\psi}, \hat{\phi}\}$, where the hatted fields are defined with the non-analytic $\sqrt{1-\rho}$ factors removed

$$\psi = \sqrt{1-\rho} \hat{\psi}, \quad (6.22a)$$

$$\phi = \sqrt{1-\rho} \hat{\phi}. \quad (6.22b)$$

6.5.3 Numerical results

Now we turn onto the discussion of our numerical results. In this section we use a grid of 60 points and work with $6 \times \text{MachinePrecision}$ in both frameworks. As for the CLMs and QNFs of $SAdS_{4+1}$ black brane, we have a divergent operator in the MS framework and we deal with that divergence as explained previously in section 6.3.3.

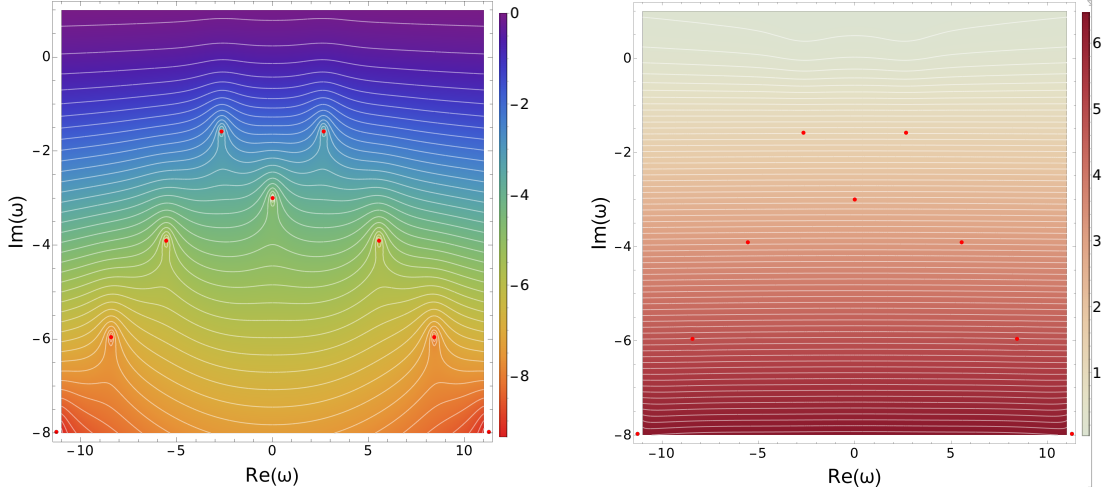


Figure 18: (Left) QNF pseudospectrum at $L = 1$ for the $SAdS_{4+1}$ black hole. The white lines denote the boundaries of different ε -pseudospectra and the heat map corresponds to the logarithm in base 10 of the inverse of the norm of the resolvent. (Right) Heatmap of the percentage difference between MS and GF frameworks. The red dots correspond to the QNFs.

For the sake of brevity we showcase results for the $L = 1$ ($\lambda^2 = L(2+L) = 3$) sector only. This is the sector with the smallest possible value of the angular momenta for

a Gauge field and thus it contains the mode closest to the real axis. In figure 18 we plot the pseudospectra and the relative difference between GF and MS frameworks. We note that as for the black brane our procedure of dealing with the divergence in the MS approach introduces numerical errors, which enhance the relative difference between MS and GF approaches. Nonetheless, for the chosen grid the maximal difference is of only 7%, which could be lowered by making the grid denser as previously discussed.

Unlike the case of the black brane, all QNFs are unstable, even the would-be hydrodynamic one (the one with no real part). This is a consequence of the large gap appearing for this mode, whose magnitude is related to the ratio l/r_h ; which we have chosen to be 1. This suggests that as the ratio l/r_h decreases and the gap is reduced we should recover the spectral stability observed for the black brane at in the small momentum limit.

7 Conclusions and outlook

In this work we have studied the stability of complex linear momenta (CLMs) and quasinormal frequencies (QNFs) of gauge fields using two different approaches: the gauge field (GF) approach and the master scalar (MS) approach.

The GF approach presents a physically well defined method to study numerically solutions of the gauge field in a determined background. In principle this method is totally inequivalent from the master scalar, presented as a not-so-well physically motivated approach to the same problem. However, we have shown that for black branes both approaches are related by Hodge duality in an effective 3-dimensional spacetime, giving physical meaning to the MS formulation.

Although recently it has been argued that ingoing Eddington Finkelstein (IEF) coordinates are better suited for numerically studying QNF pseudospectra [26, 27], we work in regular coordinates [25, 76]. Unlike in [27], we find that the convergence properties match those expected from the results of [76]. Moreover, when trying to give qualitative results in the convergent region of the pseudospectrum, IEF coordinates are ill-suited as they yield a generalized eigenvalue problem, for which the notion of stability is less transparent. In particular, this makes stable modes harder to identify.

The gauge field, and equivalently the Hodge dual scalar, present two clear advantages over the naively constructed master scalar. The first of them is that the energy norm built directly from the master scalar differs from the energy norm of the gauge field by a boundary term. In the 5-dimensional case, this term may allow for modes with negative energy, making the norm not positive definite. The other advantage comes when computing CLMs. As the master scalar approach works with a 2-dimensional scalar field, it does not present a natural way to pose the problem

of studying CLMs. In this sense, Hodge duality gives a natural way of approaching this problem as one lands on a 3-dimensional space.

As was already seen in [39] pseudospectra of QNFs and CLMs are qualitatively different. In particular the zero frequency complex momenta are normal, as they correspond to glueball masses of a dimensionally reduced theory. Here we have found, however a new phenomenon: the diffusion modes seen as a linear momentum modes show enhanced spectral instability (see also [77]). This is a direct consequence of an exceptional point sitting at zero frequency where the modes would collide. As is well known, the residue of the diffusion mode vanishes at zero frequency and strictly speaking this exceptional point is not present at $\omega = 0$. Its influence is however detectable in the pseudospectrum in a neighborhood of $\omega = 0$.

There are of course several directions in which our work has to be extended. First one should study the pseudospectra of quasinormal modes and complex momentum modes of gauge fields in asymptotically flat space using the rectangular matrix approach. Another important question is how our approach can be generalized to gravitational modes. Finding an appropriate norm in terms of the metric fields itself seems difficult since there does not exist a gauge invariant local energy momentum tensor. Nevertheless it should be quite interesting and useful to use investigate this problem further in particular in view of the role of quasinormal modes in the ringdown phase of black hole mergers. Lastly, one could also study pseudospectra in the vicinity of pole collisions. Our results for CLMs suggests that there should be an enhancement of the spectral instability as one gets close to them. Hence, pseudospectrum analysis could serve as an useful tool to diagnose them.

Acknowledgments

We thank D. Areán for valuable discussions. We thank B. Cownden, C. Pantelidou and M. Zilhão for clarifications regarding their paper. This work is supported through the grants CEX2020-001007-S and PID2021-123017NB-100, PID2021-127726NB-I00 funded by MCIN/AEI/10.13039/501100011033 and by ERDF “A way of making Europe”. The work of D.G.F. is supported by FPI grant PRE2022-101810. The work of PSB is supported by Fundación Séneca, Agencia de Ciencia y Tecnología de la Región de Murcia, grant 21609/FPI/21, Spanish MINECO grant PID2024-155685NB-C22 and Fundación Séneca de la Región de Murcia FSRM/10.13039/100007801 (22581/PI/24).

A Stability of general eigenvalue problems

As discussed in [1], one can generalize the notion of ε -pseudospectra to generalized eigenvalue problems of the form

$$(A - \lambda B)u = 0, \quad (\text{A.1})$$

with A and B differential operators. In this case one can find multiple possible definitions and should choose according to the particular problem under consideration (see e.g., Ch. 45 of [1] for a review).

In the context of gravitational physics, it has been argued in [26] that the adequate definition is given by

$$\sigma_\varepsilon(A, B) = \{z \in \mathbb{C} : \|(A - zB)^{-1}\| < 1/\varepsilon\} , \quad (\text{A.2})$$

which was proven in [82] to be equivalent to

$$\sigma_\varepsilon(A, B) = \{z \in \mathbb{C}, \exists V \text{ with } \|V\| < \varepsilon : z \in \sigma(A + V, B)\} . \quad (\text{A.3})$$

This definition indeed is the logical generalization of pseudospectra to generalized eigenvalue problems as it retains the notion of maximal region containing the eigenvalues after a perturbation. Moreover, with this definition one can define pseudospectra in infalling Eddington coordinates which were argued in [27] to show better convergence properties.

We want to stress however one important subtlety in this formulation which is often overlooked. While for a standard eigenvalue problem, a spectrally stable operator has ε -pseudospectra whose boundaries are given by circles of radius ε ; this is no longer the case for generalized eigenvalue problems. Let us illustrate this with a simple example. Take A to be the following 3×3 matrix

$$A = \text{diag}(-1, 0, 1) , \quad (\text{A.4})$$

and consider the standard euclidean inner product

$$\langle u, v \rangle_2 = \sum_{i=1}^3 u_i^* v_i . \quad (\text{A.5})$$

Then, A is a normal matrix and when studying the eigenvalue problem $(A - \lambda)u = 0$, we observe a stable ε -pseudospectra comprised of circles of radius ε , as illustrated in figure 19a. On the other hand, if we consider instead the eigenvalue problem $S(A - \lambda)u = 0$ with $S = \text{diag}(1, 3/4, 2)$, we find a qualitatively different picture as shown in figure 19b. We still observe that the ε -pseudospectrum is comprised of circles but now their radius is not only different from ε , but also not constant. Moreover, if we take a non-diagonal S

$$S = \begin{pmatrix} 1 & 0 & 1 \\ 0 & 3/4 & 4 \\ 1 & 4 & 2 \end{pmatrix} \quad (\text{A.6})$$

as in figure 19c, we see that even the circular structure is lost. However, these generalized eigenvalue problems should be equivalent to the standard one discussed

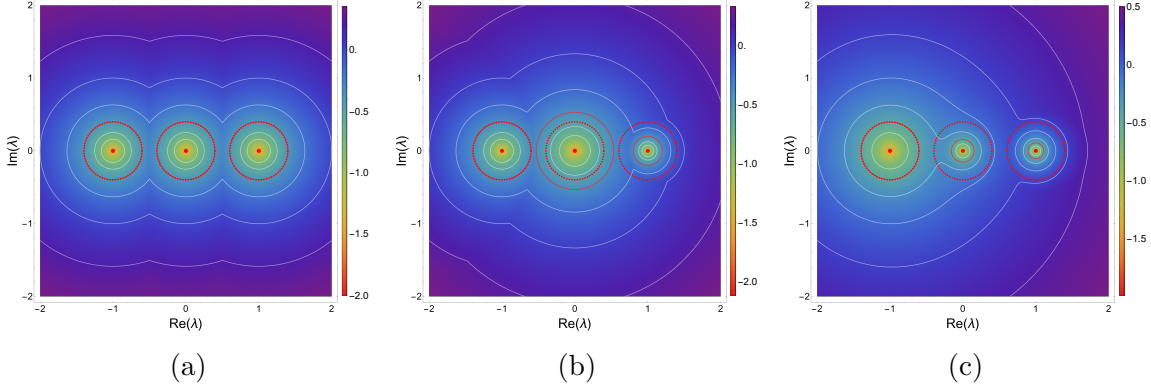


Figure 19: Pseudospectrum of $A - \lambda$ (a) and of $S(A - \lambda)$ with diagonal (b) and non-diagonal (c) S . The red dots correspond to the eigenvalues, the white lines represent the boundaries of various ε -pseudospectra, and the heat map represent to the logarithm in base 10 of the inverse of the resolvent. The solid red lines are the boundary of the $10^{-2/5}$ -pseudospectrum and the dashed red circles are circles of radius $10^{-2/5}$ centered in the eigenvalues. For (a) we see that dashed and solid lines coincide while for (b) and (c) this is no longer the case.

above. It is the non-trivial B that deforms the notion of stability. This is can be explained by the lack of invariance of the pseudospectrum under multiplication by non-unitary operators

$$\|(A - z)^{-1}\| \neq \|(SA - zS)^{-1}\|. \quad (\text{A.7})$$

We want to stress that this mismatch is not a flaw of pseudospectra, rather it is a physical feature. Clearly multiplying by a non-unitary operator changes the typical scales of the original operator, despite leaving the spectrum invariant. Thus, it makes sense that one should need larger/smaller perturbations in order to have an effect on the spectrum of the new shifted operator. This is particularly easy to understand if we take the B operator in (A.1) to be a constant. Then, clearly, a perturbation V whose effect when $B = 1$ is of order $O(1)$ will have a much smaller effect when $B = 10^6$ as its relative size is lower.

All in all, this does not mean that one should avoid generalized eigenvalue problems, or that they are ill-defined. It only suggests that one should be extra careful when interpreting pseudospectra of generalized eigenvalue problems. In particular, as seen in figure 19c, it can lead to significant confusion as the notion of stability becomes deformed. Indeed, although naively figure 19c suggest instability, in reality we know from the analysis of figure 19a that it is an artifact of the non-trivial B .¹² For this reason we advocate for the use of regular coordinates where, in most cases,

¹²An alternative viewpoint would be that multiplying by S above corresponds to a linear transformation between Hilbert spaces and that the non-trivial pseudospectrum arises from taking the norm after the transformation to be (A.5). This necessarily implies that, before the transformation

these issues can be avoided. Alternatively, one could also use a controlled case where the eigenvalues are known to be stable to calibrate (e.g. the $\omega \rightarrow 0$ limit of CLMs).

To conclude, it is worth mentioning that for rectangular eigenvalue problems, a non-trivial B matrix need not spoil the naive intuition of stability. If B is chosen such that $(A - \lambda B)$ is equivalent to a standard eigenvalue problem $(L - \lambda)$ restricted to a region of the whole function space, then the standard notion of stability is trivially inherited from that of $(L - \lambda)$. We explicitly see this in our numerical computations performed in the GF framework in section 6.

B Numerical methods

In this appendix we briefly discuss the numerical procedure allowing us to compute the pseudospectra of section 6. The core idea is to discretize the system and use theorem compute the pseudospectra of the resulting matrices. As the computation of the pseudospectra of matrices has already been explained in section 2 here we briefly discuss the discretization procedure. For a more detailed discussion we refer the reader to [7, 25]

We start by discretizing the radial direction ρ in a Chebyshev-Gauss-Lobatto grid with points

$$\rho_j = \frac{1}{2} \left[1 - \cos \left(\frac{j\pi}{N} \right) \right], \quad j = 0, 1, \dots, N, \quad (\text{B.1})$$

Then, in this grid we construct the discretized versions of our numerical operators by replacing the derivatives with the corresponding Chebyshev derivatives [83]. This corresponds to approximating the modes by sums of Chebyshev polynomials of degree N . Remarkably, as discussed in [7], consistency with the discretization, requires us to construct the energy norm in a grid with twice as many points and then interpolate it back to the original grid. This ensures that the norm is exact for polynomials of degree N . The explicit details on how to perform the interpolation can be found in [7].

Regarding the function space, as indicated in the main text we need to work in terms of the hatted variables satisfying regularity on the horizon and Dirichlet/regularity on the AdS boundary. Remarkably, as a byproduct of the discretization, regularity is immediately guaranteed as any finite sum of Chebyshev polynomials is always a regular function. On the other hand, Dirichlet boundary conditions are imposed by removing from the operators the rows and columns corresponding to the AdS boundary.

the norm cannot be (A.5) and thus alters the original notion of normality making the operator unstable and rendering the comparison between figures 19a and 19c pointless.

C Convergence of the relative difference between MS and GF approaches for AdS_{4+1}

As argued in the main text, in the setups with AdS_{4+1} asymptotics (sections 6.3-6.5), we have to deal with the divergences in the operator appearing in the MS approach in a subtle manner which introduces numerical errors which are reduced as the grid becomes denser. Hence, even if the pseudospectra do not converge (as for the QNFs) we observe that the relative difference between MS and GF approaches is lowered as the aforementioned numerical errors in the MS approach become less prominent.

In this appendix we illustrate this fact for the QNFs of the SAdS_{4+1} black brane of section 6.4. In figure 20 we plot the relative difference against the grid size N in a log-log plot for different values of the momentum k . Remarkably, we do observe that the relative difference is reduced and as N increases, with power-law behavior.

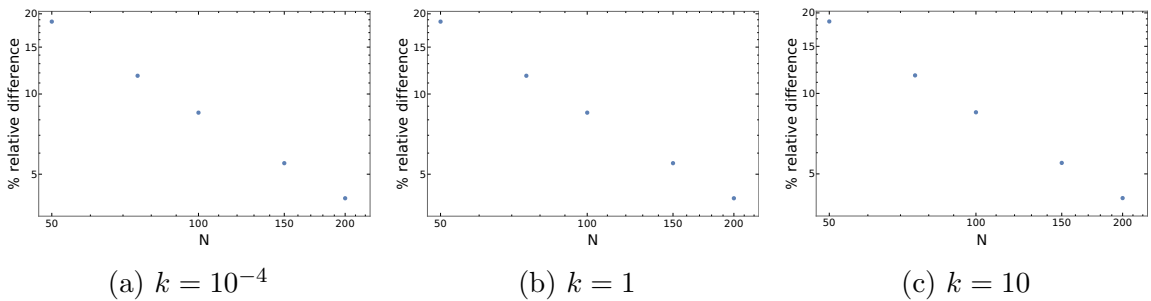


Figure 20: Relative difference as a function of the gridsize N for the QNFs of the SAdS_{4+1} black brane discussed in section 6.4 for different values of the momentum k . We find power-law behavior as indicated by the fact that the data points seem to follow straight lines in log-log scale.

D Convergence tests for QNFs and CLMs

In sections 3 and 4.2 we found that in the continuum limit the region $\text{Im}(\omega) < -\pi T$ belonged to the spectrum of the operator. Hence we argued that the pseudospectra will only converge above this band. In this section we check this prediction for the QNFs of the SAdS_{5+1} brane discussed in section 6.2, for which, in our units, $T = 5/(4\pi)$ so that the pseudospectra will converge in the region $\text{Im}(\omega) > -5/4$. In figure 21 we plot the inverse of the norm of the resolvent as a function of the grid size N evaluated at $\omega = 1i, -0.1i$ (convergent region) and at $\omega = -1.5i$ (non-convergent region). We observe that indeed the pseudospectrum converges at $\omega = -0.1i$, thus ensuring that for sufficiently small momenta, the results concerning the stability of the hydrodynamic mode are independent of N . On the other hand, for $\omega = -1.5i$ we see that the resolvent is not converging. This signals that its value tends to zero as N

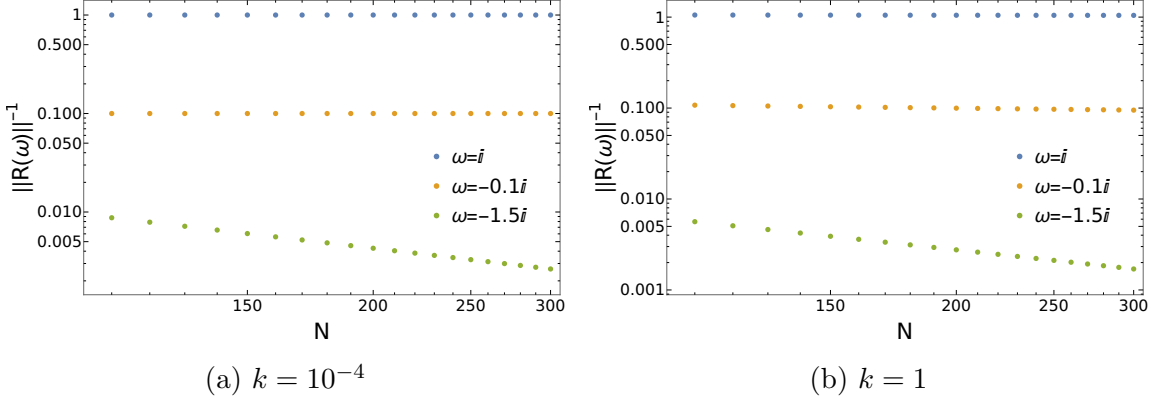


Figure 21: Inverse of the norm of the resolvent of the QNF pseudospectrum for the SAdS₅₊₁ black brane as a function of the grid size N evaluated at the representative points $\omega = \{i, -0.1i, -1.5i\}$. The results agree with the prediction that the pseudospectrum should converge in the region $\text{Im}(\omega) > -5/4$.

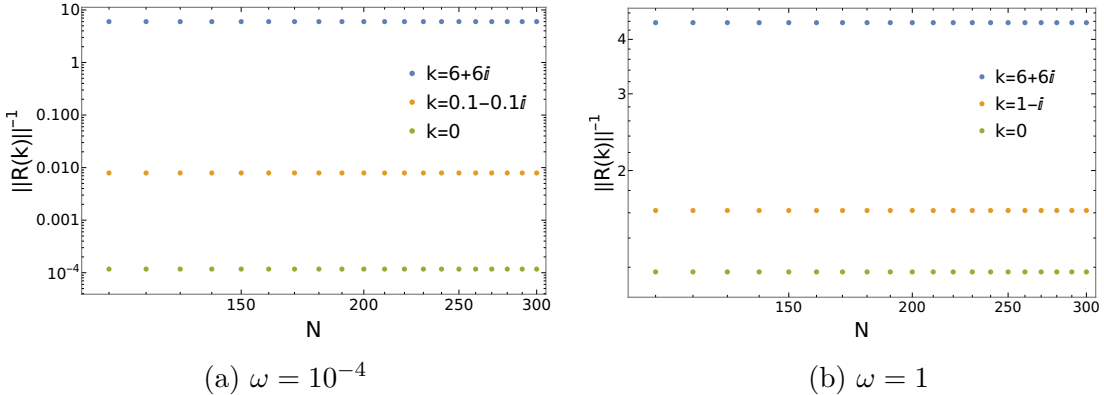


Figure 22: Inverse of the norm of the resolvent of the CLM pseudospectrum for the SAdS₅₊₁ black brane as a function of the grid size N evaluated at the representative points $k = \{6 + 6i, 1 - 1i, 0\}$. The results are convergent, in agreement with the prediction that the CLM pseudospectrum should be convergent everywhere in the complex k plane.

increases, in agreement with the fact that in the continuum limit this point belongs to the spectrum of the operator and thus the inverse of the norm of the resolvent should be zero.

It is worth mentioning that even in the region $\text{Im}(\omega) > -\pi T$, the numerical results converge more slowly the closer one gets to the line $\text{Im}(\omega) = -\pi T$. For this reason, one generically expects to need to go to very large grids to numerically identify the boundary of the convergent region.

In sections 3.1 and 5.1 we argued that the CLM pseudospectra converges everywhere as for fixed real frequency ω outgoing modes are always removed from the

spectrum. In this section we check this prediction for the CLMs of the SAdS₅₊₁ brane discussed in section 6.1. In figure 22 we plot the inverse of the norm of the resolvent as a function of the grid size N for different points in the complex momentum plane. We observe that indeed the pseudospectrum converges for all point concluding that, as argued in [39], CLMs do not suffer the convergence issues present for QNFs.

References

- [1] L. N. Trefethen and M. Embree, *Spectra and Pseudospectra*. Princeton University Press, Princeton, 2005.
- [2] J. Sjöstrand, *Non-self-adjoint differential operators, spectral asymptotics and random perturbations*, .
- [3] E. B. Davies, *Linear Operators and their Spectra*. Cambridge Studies in Advanced Mathematics. Cambridge University Press, 2007.
- [4] H.-P. Nollert, *TOPICAL REVIEW: Quasinormal modes: the characteristic ‘sound’ of black holes and neutron stars*, *Class. Quant. Grav.* **16** (1999) R159–R216.
- [5] K. D. Kokkotas and B. G. Schmidt, *Quasinormal modes of stars and black holes*, *Living Rev. Rel.* **2** (1999) 2 [[gr-qc/9909058](#)].
- [6] E. Berti, V. Cardoso and A. O. Starinets, *Quasinormal modes of black holes and black branes*, *Class. Quant. Grav.* **26** (2009) 163001 [[0905.2975](#)].
- [7] J. L. Jaramillo, R. P. Macedo and L. Al Sheikh, *Pseudospectrum and Black Hole Quasinormal Mode Instability*, *Phys. Rev. X* **11** (2021), no. 3 031003 [[2004.06434](#)].
- [8] K. Destounis, R. P. Macedo, E. Berti, V. Cardoso and J. L. Jaramillo, *Pseudospectrum of Reissner-Nordström black holes: Quasinormal mode instability and universality*, *Phys. Rev. D* **104** (2021), no. 8 084091 [[2107.09673](#)].
- [9] M. H.-Y. Cheung, K. Destounis, R. P. Macedo, E. Berti and V. Cardoso, *Destabilizing the Fundamental Mode of Black Holes: The Elephant and the Flea*, *Phys. Rev. Lett.* **128** (2022), no. 11 111103 [[2111.05415](#)].
- [10] E. Berti, V. Cardoso, M. H.-Y. Cheung, F. Di Filippo, F. Duque, P. Martens and S. Mukohyama, *Stability of the fundamental quasinormal mode in time-domain observations against small perturbations*, *Phys. Rev. D* **106** (2022), no. 8 084011 [[2205.08547](#)].
- [11] R. A. Konoplya and A. Zhidenko, *First few overtones probe the event horizon geometry*, [2209.00679](#).
- [12] L. Al Sheikh, *Scattering resonances and Pseudospectrum : stability and completeness aspects in optical and gravitational systems*. Theses, Université Bourgogne Franche-Comté, Feb., 2022.
- [13] K. Destounis and F. Duque, *Black-hole spectroscopy: quasinormal modes, ringdown stability and the pseudospectrum*, 8, 2023. [2308.16227](#).

- [14] V. Boyanov, *On destabilising quasi-normal modes with a radially concentrated perturbation*, *Front. in Phys.* **12** (2024) 1511757 [[2410.11547](#)].
- [15] R.-G. Cai, L.-M. Cao, J.-N. Chen, Z.-K. Guo, L.-B. Wu and Y.-S. Zhou, *Pseudospectrum for the Kerr black hole with spin $s=0$ case*, *Phys. Rev. D* **111** (2025), no. 8 084011 [[2501.02522](#)].
- [16] P. H. C. Siqueira, L. T. de Paula, R. Panosso Macedo and M. Richartz, *Probing the unstable spectrum of Schwarzschild-like black holes*, *Phys. Rev. D* **111** (2025), no. 10 104039 [[2501.13815](#)].
- [17] V. Boyanov, K. Destounis, R. Panosso Macedo, V. Cardoso and J. L. Jaramillo, *Pseudospectrum of horizonless compact objects: A bootstrap instability mechanism*, *Phys. Rev. D* **107** (2023), no. 6 064012 [[2209.12950](#)].
- [18] K. Destounis, M. Malato Corrêa, C. F. B. Macedo and R. Panosso Macedo, *Spectral instability of horizonless compact objects within astrophysical environments*, [2509.16310](#).
- [19] L.-M. Cao, J.-N. Chen, L.-B. Wu, L. Xie and Y.-S. Zhou, *The pseudospectrum and spectrum (in)stability of quantum corrected black hole*, [2401.09907](#).
- [20] J.-N. Chen, L.-B. Wu and Z.-K. Guo, *The pseudospectrum and transient of Kaluza–Klein black holes in Einstein–Gauss–Bonnet gravity*, *Class. Quant. Grav.* **41** (2024), no. 23 235015 [[2407.03907](#)].
- [21] L.-M. Cao, M.-F. Ji, L.-B. Wu and Y.-S. Zhou, *Pseudospectrum and time-domain analysis of the EFT corrected black holes*, *Phys. Rev. D* **112** (2025), no. 12 124022 [[2508.13894](#)].
- [22] S. Sarkar, M. Rahman and S. Chakraborty, *Perturbing the perturbed: Stability of quasinormal modes in presence of a positive cosmological constant*, *Phys. Rev. D* **108** (2023), no. 10 104002 [[2304.06829](#)].
- [23] K. Destounis, V. Boyanov and R. Panosso Macedo, *Pseudospectrum of de Sitter black holes*, *Phys. Rev. D* **109** (2024), no. 4 044023 [[2312.11630](#)].
- [24] C. Warnick, *(In)stability of de Sitter Quasinormal Mode spectra*, [2407.19850](#).
- [25] D. Areán, D. G. Fariña and K. Landsteiner, *Pseudospectra of holographic quasinormal modes*, *JHEP* **12** (2023) 187 [[2307.08751](#)].
- [26] B. Cownden, C. Pantelidou and M. Zilhão, *The pseudospectra of black holes in AdS* , *JHEP* **05** (2024) 202 [[2312.08352](#)].
- [27] V. Boyanov, V. Cardoso, K. Destounis, J. L. Jaramillo and R. Panosso Macedo, *Structural aspects of the anti-de Sitter black hole pseudospectrum*, *Phys. Rev. D* **109** (2024), no. 6 064068 [[2312.11998](#)].
- [28] J. Carballo and B. Withers, *Transient dynamics of quasinormal mode sums*, *JHEP* **10** (2024) 084 [[2406.06685](#)].

[29] J. Carballo, C. Pantelidou and B. Withers, *Non-modal effects in black hole perturbation theory: transient superradiance*, *JHEP* **08** (2025) 179 [[2503.05871](#)].

[30] A. Courty, K. Destounis and P. Pani, *Spectral instability of quasinormal modes and strong cosmic censorship*, *Phys. Rev. D* **108** (2023), no. 10 104027 [[2307.11155](#)].

[31] J. L. Jaramillo, R. Panosso Macedo and L. A. Sheikh, *Gravitational Wave Signatures of Black Hole Quasinormal Mode Instability*, *Phys. Rev. Lett.* **128** (2022), no. 21 211102 [[2105.03451](#)].

[32] J. L. Jaramillo, *Pseudospectrum and binary black hole merger transients*, *Class. Quant. Grav.* **39** (2022), no. 21 217002 [[2206.08025](#)].

[33] Y.-S. Zhou, M.-F. Ji, L.-B. Wu and L.-M. Cao, *Pseudospectrum and black hole total transmission mode (in)stability*, [2512.16372](#).

[34] N. Andersson and K. E. Thylwe, *Complex angular momentum approach to black hole scattering*, *Class. Quant. Grav.* **11** (1994) 2991–3001.

[35] I. Amado, C. Hoyos-Badajoz, K. Landsteiner and S. Montero, *Absorption lengths in the holographic plasma*, *JHEP* **09** (2007) 057 [[0706.2750](#)].

[36] T. Torres, *From Black Hole Spectral Instability to Stable Observables*, *Phys. Rev. Lett.* **131** (2023), no. 11 111401 [[2304.10252](#)].

[37] R. F. Rosato, K. Destounis and P. Pani, *Ringdown stability: greybody factors as stable gravitational-wave observables*, [2406.01692](#).

[38] N. Oshita, K. Takahashi and S. Mukohyama, *(In)stability of the black hole greybody factors and ringdowns against a small-bump correction*, [2406.04525](#).

[39] D. Garcia-Fariña, K. Landsteiner, P. G. Romeu and P. Saura-Bastida, *Pseudospectra of complex momentum modes*, *JHEP* **01** (2025) 185 [[2407.06104](#)].

[40] L.-B. Wu, R.-G. Cai and L. Xie, *Stability of the greybody factor of Hayward black holes*, *Phys. Rev. D* **111** (2025), no. 4 044066 [[2411.07734](#)].

[41] R. F. Rosato, S. Biswas, S. Chakraborty and P. Pani, *Excitation factors for horizonless compact objects: long-lived modes, echoes, and greybody factors*, [2511.08692](#).

[42] L. Xie, L.-B. Wu and Z.-K. Guo, *Spectrum instability and graybody factor stability for parabolic approximation of Regge-Wheeler potential*, *Phys. Rev. D* **112** (2025), no. 2 024054 [[2505.21303](#)].

[43] J. M. Maldacena, *The Large N limit of superconformal field theories and supergravity*, *Adv. Theor. Math. Phys.* **2** (1998) 231–252 [[hep-th/9711200](#)].

[44] O. Aharony, S. S. Gubser, J. M. Maldacena, H. Ooguri and Y. Oz, *Large N field theories, string theory and gravity*, *Phys. Rept.* **323** (2000) 183–386 [[hep-th/9905111](#)].

[45] M. Ammon and J. Erdmenger, *Gauge/gravity duality: Foundations and applications*. Cambridge University Press, Cambridge, 4, 2015.

[46] J. Zaanen, Y. Liu, Y. Sun and K. Schalm, *Holographic Duality in Condensed Matter Physics*. Cambridge University Press, 2015.

[47] S. A. Hartnoll, A. Lucas and S. Sachdev, *Holographic Quantum Matter*. MIT Press, 2018.

[48] G. T. Horowitz and V. E. Hubeny, *Quasinormal modes of AdS black holes and the approach to thermal equilibrium*, *Phys. Rev. D* **62** (2000) 024027 [[hep-th/9909056](#)].

[49] D. Birmingham, I. Sachs and S. N. Solodukhin, *Conformal field theory interpretation of black hole quasinormal modes*, *Phys. Rev. Lett.* **88** (2002) 151301 [[hep-th/0112055](#)].

[50] P. K. Kovtun and A. O. Starinets, *Quasinormal modes and holography*, *Phys. Rev. D* **72** (2005) 086009 [[hep-th/0506184](#)].

[51] G. Policastro, D. T. Son and A. O. Starinets, *The Shear viscosity of strongly coupled $N=4$ supersymmetric Yang-Mills plasma*, *Phys. Rev. Lett.* **87** (2001) 081601 [[hep-th/0104066](#)].

[52] R. Baier, P. Romatschke, D. T. Son, A. O. Starinets and M. A. Stephanov, *Relativistic viscous hydrodynamics, conformal invariance, and holography*, *JHEP* **04** (2008) 100 [[0712.2451](#)].

[53] S. Bhattacharyya, V. E. Hubeny, S. Minwalla and M. Rangamani, *Nonlinear Fluid Dynamics from Gravity*, *JHEP* **02** (2008) 045 [[0712.2456](#)].

[54] P. Kovtun, D. T. Son and A. O. Starinets, *Viscosity in strongly interacting quantum field theories from black hole physics*, *Phys. Rev. Lett.* **94** (2005) 111601 [[hep-th/0405231](#)].

[55] S. S. Gubser, *Breaking an Abelian gauge symmetry near a black hole horizon*, *Phys. Rev. D* **78** (2008) 065034 [[0801.2977](#)].

[56] S. A. Hartnoll, C. P. Herzog and G. T. Horowitz, *Building a Holographic Superconductor*, *Phys. Rev. Lett.* **101** (2008) 031601 [[0803.3295](#)].

[57] I. Amado, M. Kaminski and K. Landsteiner, *Hydrodynamics of Holographic Superconductors*, *JHEP* **05** (2009) 021 [[0903.2209](#)].

[58] C. P. Herzog and S. S. Pufu, *The Second Sound of $SU(2)$* , *JHEP* **04** (2009) 126 [[0902.0409](#)].

[59] C. P. Herzog, P. Kovtun, S. Sachdev and D. T. Son, *Quantum critical transport, duality, and M-theory*, *Phys. Rev. D* **75** (2007) 085020 [[hep-th/0701036](#)].

[60] M. Cubrovic, J. Zaanen and K. Schalm, *String Theory, Quantum Phase Transitions and the Emergent Fermi-Liquid*, *Science* **325** (2009) 439–444 [[0904.1993](#)].

[61] N. Iqbal, H. Liu and M. Mezei, *Lectures on holographic non-fermi liquids and quantum phase transitions*, in *String Theory and Its Applications*, WORLD SCIENTIFIC, Nov., 2011.

[62] S. Grozdanov, K. Schalm and V. Scopelliti, *Black hole scrambling from hydrodynamics*, *Phys. Rev. Lett.* **120** (2018), no. 23 231601 [[1710.00921](#)].

[63] M. Blake, R. A. Davison, S. Grozdanov and H. Liu, *Many-body chaos and energy dynamics in holography*, *JHEP* **10** (2018) 035 [[1809.01169](#)].

[64] I. Amado, C. Hoyos-Badajoz, K. Landsteiner and S. Montero, *Hydrodynamics and beyond in the strongly coupled $N=4$ plasma*, *JHEP* **07** (2008) 133 [[0805.2570](#)].

[65] K. Landsteiner, *The Sound of Strongly Coupled Field Theories: Quasinormal Modes In AdS*, *AIP Conf. Proc.* **1458** (2012), no. 1 174–189 [[1202.3550](#)].

[66] L. Gavassino, M. M. Disconzi and J. Noronha, *Dispersion relations alone cannot guarantee causality*, [2307.05987](#).

[67] E. Witten, *Anti-de Sitter space, thermal phase transition, and confinement in gauge theories*, *Adv. Theor. Math. Phys.* **2** (1998) 505–532 [[hep-th/9803131](#)].

[68] C. Csaki, H. Ooguri, Y. Oz and J. Terning, *Glueball mass spectrum from supergravity*, *JHEP* **01** (1999) 017 [[hep-th/9806021](#)].

[69] R. de Mello Koch, A. Jevicki, M. Mihailescu and J. P. Nunes, *Evaluation of glueball masses from supergravity*, *Phys. Rev. D* **58** (1998) 105009 [[hep-th/9806125](#)].

[70] R. C. Brower, S. D. Mathur and C.-I. Tan, *Glueball spectrum for QCD from AdS supergravity duality*, *Nucl. Phys. B* **587** (2000) 249–276 [[hep-th/0003115](#)].

[71] D. Bak, A. Karch and L. G. Yaffe, *Debye screening in strongly coupled $N=4$ supersymmetric Yang-Mills plasma*, *JHEP* **08** (2007) 049 [[0705.0994](#)].

[72] J. Sonner and B. Withers, *Universal spatial structure of nonequilibrium steady states*, *Phys. Rev. Lett.* **119** (2017), no. 16 161603 [[1705.01950](#)].

[73] I. Novak, J. Sonner and B. Withers, *Overcoming obstacles in nonequilibrium holography*, *Phys. Rev. D* **98** (2018), no. 8 086023 [[1806.08655](#)].

[74] M. P. Heller, A. Serantes, M. Spaliński, V. Svensson and B. Withers, *Hydrodynamic gradient expansion in linear response theory*, *Phys. Rev. D* **104** (2021), no. 6 066002 [[2007.05524](#)].

[75] R. A. Janik, M. Jarvinen and J. Sonnenschein, *A simple description of holographic domain walls in confining theories — extended hydrodynamics*, *JHEP* **09** (2021) 129 [[2106.02642](#)].

[76] C. M. Warnick, *On quasinormal modes of asymptotically anti-de Sitter black holes*, *Commun. Math. Phys.* **333** (2015), no. 2 959–1035 [[1306.5760](#)].

[77] L.-M. Cao, M.-F. Ji, L.-B. Wu and Y.-S. Zhou, *Exceptional line and pseudospectrum in black hole spectroscopy*, [2511.17067](#).

[78] T. Kato, *Perturbation theory for linear operators*, vol. 132. Springer Science & Business Media, 2013.

[79] D. H. Richard Courant, *Methods of Mathematical Physics Volume 1*. Wiley-VCH, 1 ed., 1989.

- [80] L. Hui, A. Joyce, R. Penco, L. Santoni and A. R. Solomon, *Static response and Love numbers of Schwarzschild black holes*, *JCAP* **04** (2021) 052 [[2010.00593](https://arxiv.org/abs/2010.00593)].
- [81] I. R. Klebanov and E. Witten, *AdS / CFT correspondence and symmetry breaking*, *Nucl. Phys. B* **556** (1999) 89–114 [[hep-th/9905104](https://arxiv.org/abs/hep-th/9905104)].
- [82] J. L. M. Van Dorsselaer, *Pseudospectra for matrix pencils and stability of equilibria*, *BIT Numerical Mathematics* **37** (1997), no. 4 833–845.
- [83] L. N. Trefethen, *Spectral Methods in MATLAB*. Society for Industrial and Applied Mathematics, USA, 2000.